CHAPTER
ONE

MACROSTRUCTURE

1-1 INTRODUCTION

Macroscopic examination techniques are frequently employed in routine quality control, in failure analysis, and in research studies. These techniques are generally a prelude to microscopic examination; however, in quality control, they are often used alone as a criterion for acceptance or rejection. A great variety of destructive and nondestructive procedures are available. The most basic procedure involves simple visual examination for surface features such as seams, laps, or scale.

This chapter describes only destructive test procedures; nondestructive methods are not covered. These destructive methods include the following procedures:

- Macroetching
- Contact printing
- Fracturing
- Lead exudation

Proper implementation of these methods is fundamental to the manufacture of materials. In quality control, the manufacturing routine is usually established according to set practices, and the macroscopic methods are used to detect deviations from the norm. In failure studies, one often does not know specific details of the manufacturing process and practices, and the engineer uses these tests to judge quality, to locate problem areas for further study, and, in some cases, to determine how the component was produced. In research studies, the processing steps are often varied, and the macroexamination is designed to show differences due to changes in manufacturing practices. Thus for each type of study, the specific details of the macroscopic examination will vary somewhat, and

tallography Prin
George F. Vander
DOI: 10.1361/mp

the practitioner must have a thorough understanding of the test method, its application, and the interpretation of test data.

Interpretation of the data from these tests requires an understanding of the manufacturing process, since the macrostructure is dependent on the solidification and hot- or cold-working procedures used. There can be pronounced differences in macrostructure because factors such as casting method, ingot size and shape, and chemical analysis will significantly alter the solidification pattern. In addition, the use of manufacturing techniques other than traditional ingot casting, such as continuous casting, centrifugal casting, electroslag remelting, or hot-isostatic pressing, produce noticeably different as-cast patterns. Also, there is a wide variety of metalworking processes that can be applied to material made by any of the above processes, and each exerts a different effect upon the material. All these factors influence the interpretation of the test results.

No material can be said to be entirely homogeneous either macroscopically or microscopically. The degree of heterogeneity can vary widely depending on the nature of the material, the method of manufacture, and the cost required to produce the material. Fortunately, the usual degree of heterogeneity is not a serious problem in the use of commercial materials as long as these variances are held within certain prescribed limits. Certain problems, such as pipe and hydrogen flakes, are in general, quite harmful. The effect of other features, such as porosity, segregation, and inclusions, can be quite difficult to evaluate, and one must consider the extent of these features, the amount of subsequent metalworking, and the nature of the application of the material.

Of the metallographic procedures listed, the macroetch test is probably the most informative, and it is widely used for quality control, failure analysis, and research studies. Classification of the features observed with the macroetch test is often confusing because of the use of "jargon" created since the introduction of this test procedure. The macroetch test is covered in considerable detail in this chapter, and numerous examples of its application to a variety of materials are presented.

1-2 VISUALIZATION AND EVALUATION OF MACROSTRUCURE BY ETCHING

All quality evaluations should begin on the macroscale using tests designed to survey the overall field in a simple and reliable manner. After the macrostructure of a material has been evaluated, specific features can then be examined microscopically. Abnormalities observed on the etch disc can be studied by fracturing the disc or by preparing metallographic polished samples. Macroetching of transverse or longitudinally oriented samples, i.e., oriented with respect to the hot-working axis, enables the mill metallurgist to evaluate the quality of a relatively large area quickly and efficiently. Thus, macroetching is an extremely powerful tool and is a cornerstore of the overall quality program.

The earliest macroetchants were rather weak solutions used at room temperature. Reaumur (1683–1757) used macroetchants to distinguish between different types of steel and sketched the appearance of macroetched pieces of steel in his work. Rinmann promoted this technique in his book *On the Etching of Iron and Steel,* written in the late 1700s. Sorby, in his classic work published in 1887 "On the Microscopical Structure of Iron and Steel," showed "nature prints," which were inked contact prints of steel etched in moderately strong aqueous nitric acid solutions [1]. The early etching solutions have been reviewed in the classic text by Berglund [2].

1-2.1 Macroetching with Acid Solutions

The first "deep"-etching procedure for steel was developed by Waring and Hofamman using nine parts hydrochloric acid, three parts sulfuric acid, and one part water. Considerable adverse comment about the use of strong acids to evaluate highly stressed components was generated by this paper. Overall, the initial response to deep-acid etching was negative; however, numerous subsequent studies revealed the great value of such etchants.

After the initial work by Waring and Hofamman, considerable attention was devoted to the study of strong acids for deep etching steels. The most widely used deep etch consists of a 1:1 solution of reagent-grade† hydrochloric acid and water heated to 160 to 180°F for 15 to 45 min. Etching can be conducted on a saw-cut face, but better resolution is obtained with ground faces. Gill and Johnstin found that this etch was more selective in its attack than similar solutions involving nitric acid and water or sulfuric acid and water [3]. An important feature of this etchant is that evaporation does not significantly vary its composition during use.

The following items should be considered in the development of a macroetchant:

- The etchant should produce good all-around results, should be applicable to the majority of materials, and should reveal a great variety of structural characteristics and irregularities.
- The etchant should be simple in composition, inexpensive, and easy to prepare.
- The etchant should be stable during use or storage.
- The etchant must be safe to use and should not produce noxious odors.

The widespread popularity of the 1:1 hydrochloric acid and water etch is due to the fact that it satisfies these requirements better than other etchants. Appendix A lists macroetchants for iron and steel as well as for other metals.

The 1:1 hydrochloric acid and water etch attacks manganese sulfides readily but does not attack aluminum oxides. Steels high in aluminum content, such as the nitriding alloys, are etched best with an aqueous solution containing 10% hydro-

†The reagent grade contains 36.5 to 38% HCl, whereas the technical grade contains 28% HCl

chloric acid and 2% nitric acid, developed by V. T. Malcolm. Etching is conducted at 180°F for 15 to 60 min.

As the alloy content increases, so does the degree of segregation and its associated problems. Etching is pronounced at the segregate-matrix interface, and segregate or matrix areas may etch out, leaving pits. Sulfides or carbides may also etch out, leaving pits. Before the investigator can distinguish between pits due to nonmetallic inclusions or segregates and carbides, the disc must be hardened and reetched. If the pits were due to nonmetallics, they will be present to the same degree in both the annealed and the hardened discs.

Watertown Arsenal [4] developed a variant of the standard etch that consists of 38 parts of hydrochloric acid, 12 parts sulfuric acid, and 50 parts water.† This reagent often produces a sharper definition of features than the standard etch, and like the standard etch, its acid concentration does not change markedly during use.

Macroetching provides an overall view of the degree of uniformity of metals and alloys by revealing:

- Structural detail resulting from solidification or working
- Chemical uniformity in qualitative terms
- Physical discontinuities due to solidification, working, etc.
- Weldment structure or heat-affected zones from burning operations
- Hardness patterns in non-through-hardened steels or patterns due to quenching irregularities
- Grinding damage
- Thermal effects due to service abuse

The first three features are best revealed by hot-acid etching, and the remaining four are best revealed by room temperature etchants. Macroetching is usually performed on ground surfaces, although in some cases, especially with cold etchants, better results are obtained when the surface is polished. Chemical segregation can be shown by certain cold etchants. The information obtained can be recorded by photographing the samples or, where possible, by contact printing.

In order to observe these features, one must sample the material properly and use the macroetch test procedure correctly. Fortunately, these test procedures are straightforward and simple to use as long as a few precautions are followed. In practice, one must consider the following test variables:

- Selection of representation samples
- Choice of surface orientation
- Proper preparation of sample surface
- Selection of the best etch composition
- Control of etchant temperature and etch time
- Documentation of test results

†Add the sulfuric acid *slowly* to the water and allow it to cool; then add the hydrochloric acid.

For routine mill inspection, the metallurgist generally cuts a disc from the top and bottom (occasionally the middle) of billets rolled from the first, middle, and last ingots. For certain products, discs are prepared from all the ingots, after rolling to the required billet size. These discs should be cut so as not to include any of the shear drag which may be present after hot shearing the billets to length or removing the top and bottom discard material. In general, the thickness should be held to ½ to 1 in, since the weight of larger discs is prohibitive for handling. Both cuts should be relatively parallel. It is advisable to cut discs with large cross sections into two or more pieces; cutting directly through the center of the disc should be avoided. Transverse discs are used in most cases, although longitudinal discs can be useful in evaluating segregation and mechanical heterogeneity. For routine work with steels, the saw-cut face is generally satisfactory for etching. For detection of fine details, a smooth ground surface is preferred. Some etchants require a smooth ground or a polished surface for proper delineation of macroetch features.

It is not necessary to remove the as-rolled scale from the disc, but any grease, dirt, or debris on the cut face should be removed. It is not advisable to hot-acid etch hardened steel discs, since they can crack or fracture during etching. Similarly, billets should be soft prior to cutting to prevent surface damage during cutting which will obscure the true etch pattern. Proper cutting and grinding techniques must be employed to avoid any damage from these sources.

1-2.2 Copper-Containing Macroetchants for Primary Structure

Macroetching steels with etchants containing copper ions predates the development of hot-acid etching. These copper-containing reagents are listed in App. B. Heyn's reagent was the first to be developed; some of the others stemmed from efforts to produce better results. The reagents are used principally to reveal phosphorus or carbon segregation and dendritic structure. At the time these reagents were first introduced, phosphorus segregation was an important problem in Bessemer steels. Today, however, little Bessemer steel is produced and phosphorus segregation is not a major problem. However, carbon segregation is still widely evaluated, especially in high-carbon steels. These etchants are employed primarily now in research studies and occasionally in quality control. One of the uses of these etchants has been to reveal the primary structure of materials, that is the gross structure resulting from solidification rather than the secondary or tertiary microstructure. More recently developed copper-containing macroetchants have been used to study strain patterns in stressed metals.

Stead's no. 1 reagent is one reagent that has been widely used. Stead recommended that the etch be used in the following way: A small amount of the etching solution is poured on the surface, and etching is allowed to proceed for about 1 min. The solution is drained off, and fresh solution is added. This process is repeated until the desired etch pattern is obtained. Magnusson [5] states that this procedure produces uneven etching across the sample and results are better if the specimen is etched by immersion, which is contrary to Stead's comment that immersion should never be used.

Magnusson has performed an exhaustive study of the use of Stead's reagent for revealing the primary structure of welds [5]. Magnusson states that the influence of the secondary and tertiary structure must be reduced so that the primary structure can be clearly observed. This can be accomplished by heat treating the specimen prior to etching. While normalizing produces improved results, best results are obtained by quenching and tempering. He recommends austenitizing at about 125°F (52°C) above the upper critical temperature. After a short (5 min) hold, the sample is quenched fast enough to form martensite and is tempered between about 1025 and 1250°F (552 and 677°C) for 1 h. Tempering above 1250°F produces indistinct contrast.

Stead's reagent is used with polished surfaces. According to Magnusson, after heat treatment the sample should be polished using nital etching between the final polishing steps. After the final polishing stage, the sample should be etched about 5 s in 0.5% nital. The sample is rinsed and dried and then etched by immersion. Etching is started with a solution of one part Stead's reagent plus three parts alcohol and one-quarter part water for 45 s. The sample is rinsed, and 5 to 10 drops of a 50-mL solution of 10% ammonia plus 10 drops of H_2O_2 is poured on the surface. The copper precipitate is removed by wiping with cotton. The sample is then etched twice for 30 s (rinse and dry between etches) in one part Stead's reagent and two parts alcohol and then in dilute Stead's reagent (dilution not specified, probably one part alcohol) for 15 s. Preetching with picral produces softer contrast. Magnusson also recommends preetching with a solution of 10 mL of 0.5% HNO_3 plus three drops of 4% picral for improved contrast.

Oberhoffer's reagent has also been widely used because of the good, uniform results obtained. However, well-polished surfaces must be used and best results are obtained if the polished surface is left to sit in air for about 1 h before etching, as pointed out by Magnusson. Pokorny has made a detailed study of the influence of the surface condition, using copper-containing reagents as the macroetchant [6]. Polishing produces two surface effects, a mechanically deformed layer and a chemically absorbed layer. Pokorny claims that primary etching works best in the presence of these two layers. Most other studies claim that the mechanically deformed layer must be removed. The chemically absorbed layer was studied after diamond and alumina polishing using AES (auger electron spectroscopy) and SIMS (secondary ion mass spectrometry) techniques, which showed that this layer consisted of oxygen-metal compounds plus sulfur or ammonium compounds, depending on whether polishing was conducted in an urban or a rural atmosphere. The chemical layer can be removed by ion bombardment. A clean metallic surface is obtained after removal of about 4 nm.

Pokorny showed that etching of freshly polished surfaces produced average results, while samples etched after standing in air or in a vacuum for 20 h produced very good results. He recommends that diamond polishing be conducted only long enough to remove the scratches from grinding and then the samples be aged in air before etching.

Buhr and Weinberg compared the results obtained with the standard 1 : 1 HCl and H_2O hot etch and with Oberhoffer's reagent to autoradiographs of direction-

ally solidified AISI (American Iron and Steel Institute) 4340 doped with radioactive phosphorus [7]. This work stemmed from the statement of Kirkaldy et al. that Oberhoffer's reagent was unsuitable as a detector of phosphorus segregation. Both studies agreed that Oberhoffer's reagent would not produce a useful correlation between the rate of copper deposition and the alloy content. They observed that the hot-HCl etch brought out the outline of the dendrites but little else, did not reveal secondary branches, and attacked the phosphorus-rich regions. Oberhoffer's etch deposited copper preferentially on the phosphorus-depleted regions and delineated the phosphorus segregation fairly well. The phosphorus-depleted secondary branches were barely revealed, and the widths of these branches were similar to those revealed by the autoradiograph.

Buhr and Weinberg observed that copper was initially deposited preferentially on the phosphorus-depleted regions [7]. Then, a secondary etching attack occurred in these regions that was apparently associated with the structure, producing deeply etched acicular dark areas. This attack produced the dark appearance of the dendrite branches.

These authors studied the influence of carbon content on the action of Oberhoffer's reagent using the following steels:

	Weight %				
Code	C	P	Mn	Si	S
A	0.01	0.001	0.39	0.33	0.004
B	0.01	0.061	0.37	0.33	0.004
C	0.46	0.001	0.52	0.31	0.007
D	0.45	0.053	0.10	0.28	0.007

Steels A and C with low phosphorus content did not exhibit a dendritic pattern when etched with Oberhoffer's reagent. Steel B showed a slight indication, while Steel D exhibited a well-delineated dendritic pattern. These results clearly showed that carbon must be present along with sufficient phosphorus for the dendritic structure to be revealed. The influence of phosphorus level was also examined using AISI 4340 castings with 0.006, 0.020, 0.043, and 0.090% phosphorus. All four samples exhibited dendrite patterns after etching, with the pattern being more pronounced as the phosphorus level increased. According to Karl, the lower limit of phosphorus detection using Oberhoffer's reagent is 0.003% [8].

1-2.3 Macroetchants for Revealing Strain Patterns

In 1921, Fry published a method for revealing strain lines in iron and steel using both microscopic and macroscopic etching reagents. The macroetchant, Fry's

no. 4 (see App. B), has been widely used. This solution contains considerable hydrochloric acid, which keeps the free copper from depositing on the sample during etching. A polished specimen is immersed in the solution for 1 to 3 min. It is then removed from the solution, and etching is continued by rubbing with a cloth moistened in the solution and covered with $CuCl_2$.† This is continued for 2 to 20 min. The surface should be washed in alcohol (water should not be used for washing) and dried periodically for inspection. If the surface is not bright, rubbing is continued. Etching produces a pattern of light and dark bands corresponding to the location of the maximum shear stresses.

It is recommended that the samples be aged between 400 and 500°F for about 30 min prior to etching. If the etched surface appears dirty, it should be wiped with a cloth saturated with the etching solution. After etching, it is helpful to rinse the specimen in a fairly concentrated solution of hydrochloric acid. The sample can then be safely washed with water and dried. In addition to strain lines, the etch may produce grain contrast.

The studies of Koster [9] and MacGregor and Hensel [10] were instrumental in showing why some steels respond to Fry's reagent while others do not. Koster claimed that the variability in etch response was due to the effect of the aging treatment. Koster believed that Fry's reagent worked only after iron nitride was precipitated during aging. The nitrogen content and the form in which nitrogen is found is critical. Steels high in nitrogen content, such as Bessemer steels, etch readily in a few minutes, while open-hearth steels with lower nitrogen content require several hours or more to reveal the strain pattern. Steels with still lower nitrogen levels cannot be successfully etched. MacGregor and Hensel state that mild steels with 0.01 to 0.05% nitrogen are readily etched with Fry's reagent. They showed that a steel with low nitrogen content that would not respond to Fry's reagent could be successfully etched after light nitriding of the polished surface.

Bish has developed a method to reveal strain patterns in mild steel with low nitrogen content using a modification of Fry's reagent on mild steel plates deformed by punching [11, 12]. The surface is ground to remove about 1 mm of metal and then ground on coarse emery cloth with paraffin lubrication and then with 150-, 220-, 400-, and 600-grit SiC paper with water for the lubricant. The surface is next chemically polished in a solution consisting of 60 mL of H_2O_2, 140 mL of water, and 10 mL of HF. The sample is first degreased and then swabbed in the chemical polish for 10 s. It is then rinsed in water and dipped in a 20 to 50% solution of HCl in water, rinsed and dried. The specimen is then etched in the modified Fry's reagent by swabbing and immersion using a solution consisting of 36 g of $CuCl_2$, 144 mL of HCl, and 80 mL of water. A black deposit forms on the specimen and is removed by immersing the sample in the chemical polishing solution. This procedure also increases the contrast between the deformed and undeformed regions. The sample is next rinsed in water and dipped again in the dilute HCl solution, then rinsed and dried. Only analytical-grade HCl should be used for making up the solutions described by Bish. Bish claims that successful

† Use plastic gloves when performing this step of the process.

etching requires the removal of any surface damage produced during sectioning and grinding and the use of the chemical polish to remove damage from fine grinding. The chemical polish also appears to produce an active surface. Bish states that this procedure produces etching of the undeformed regions rather than the deformed regions, as is normally observed.

Macroetching procedures have also been developed to reveal strain patterns in nonferrous metals. Procedures for aluminum and nickel-base superalloys are given in App. C.

The strain pattern in most metals can be revealed by annealing the specimen after deformation so as to obtain recrystallization [13]. In the region that receives a critical amount of strain, generally 5 to 8 percent, grain growth is more rapid. This area shows up quite clearly upon macroetching.

1-2.4 Macroetch Specifications

The classification of macrostructures as a basis for acceptance or rejection of materials has been worked out and is now fairly straightforward. Serious defects and very good macrostructures are easily interpreted. In the case of the questionable macrostructure, however, the investigator must have experience and knowledge of the manufacturing procedures and the intended application before the macrostructure can be correctly classified. If the tested section is to be hot-worked to a smaller cross section, the mill metallurgist must know whether the additional hot work will improve the macrostructure sufficiently. Alternatively, rolling the bloom to a smaller size than originally desired in order to obtain a salable product must occasionally be recommended.

The American Society for the Testing of Materials (ASTM) has had a long involvement with macroetching techniques. The macroetching solutions for both ferrous and nonferrous metals were recently incorporated in a single specification, ASTM E340. ASTM has also developed specifications for evaluating the macrostructure of steels. In 1948, ASTM Specification A317, "Standard Method of Macroetch Testing and Inspection of Steel Forgings," was proposed. This specification showed macrographs that illustrated common features revealed by macroetching.

The first rating chart for macrostructure was published in 1957 as MIL-STD-430, "Macrograph Standards for Steel Bars, Billets and Blooms." This rating chart consisted of four series with eight macroetch pictures arranged in increasing order of severity:

Code	Type indication
A	Center defects
B	Subsurface defects
C	Ring defects
D	Miscellaneous defects (inclusions, flakes, and bursts)

The D category contained independent examples of particular types of imperfections. This chart is used in MIL-STD-1459A (MU), "Military Standard—Macrograph Standards for Steel Bars, Billets and Blooms for Ammunition Components."

MIL-STD-430 was revised, and the rating chart was changed in MIL-STD-430A. Two charts are used; the first chart shows three series of macroetch pictures with five picture per series:

Code	Type indication
S	Subsurface conditions
R	Random conditions
C	Center segregation

The second chart shows an example of a ring pattern which is judged acceptable in any degree and five examples of defects which are unacceptable in any degree (flute cracks, gas, butt tears, splash, and flakes). Both of these charts were adopted in 1968 in ASTM E381, "Standard Method for Rating Macroetched Steel."

In 1971, ASTM approved Specification A561, "Standard Recommended Practice for Macroetch Testing of Tool Steel Bars." This specification has a rating chart with two categories—ring pattern and center porosity—with six pictures per category. Another recently developed macroetch standard is ASTM A604, "Standard Method for Macroetch Testing of Consumable Electrode Remelted Steel Bars and Billets," adopted in 1970. This chart was developed to categorize and rate macroetch imperfections that are unique to these materials. Five examples of each class of macroetch imperfection are provided, with the severity increasing from A to E.

Class	Type indication
1	Freckles
2	White spots
3	Radial segregation
4	Ring pattern

These macroetch rating methods can be applied in a variety of ways. Steels made according to specific ASTM standards can be tested according to ASTM-agreed limits, implied industry limits, or producer-purchaser limits. Some ASTM standards state the chart method that is used but do not list macroetch limits. Other ASTM material specifications require macroetch tests but do not recommend a specific chart method.

1-2.5 Classification of Macroetch Features

Macroetching reveals many types of detail pertinent to the manufacturing process. It is important to categorize these defects and imperfections using unambiguous, universally understood terminology. Unfortunately, mill metallurgists do not all use the same jargon when describing macroetching features, which produces some confusion. The following lists the defects and imperfections associated with specific types of products.

1. Macroscopic features in castings
   a. *Blowholes.* Round or elongated, smooth-walled cavities that are due to entrapped air or gas generation from molding or core sand and inadequate venting.
   b. *Cold shut (cold lap).* An interface caused by lack of fusion between two streams of metal during die casting due to inadequate fluidity.
   c. *Contraction crack (hot tear).* A crack formed during cooling. The crack location is fixed by the casting design and contraction resistance due to the mold or cores.
   d. *Gas holes (pinholes).* Small, uniformly distributed spherical cavities with bright walls, due to gas evolution.
   e. *Oxide and dross inclusions.* Macroscopic included matter entrapped in the castings that results from the entry of slag or dross into the casting during pouring.
   f. *Sand holes.* Irregularly shaped cavities containing entrapped sand from the mold.
   g. *Shrinkage cavity.* Irregularly shaped cavities within the casting that are due to inadequate feeding.
   h. *Shrinkage porosity.* Irregularly shaped pores usually observed at a change of section or at the center of heavy sections that are due to inadequate feeding.
2. Macroscopic features in wrought ingot products
   a. *Surface defects such as seams or laps.* Seams are perpendicular to the bar surface and follow the hot-working axis. Laps are developed during hot working by the folding over of surface metal.
   b. *Pipe.* A remnant of the ingot-solidification cavity usually associated with segregated impurities. In so-called primary pipe, the cavity is opened to the atmosphere and the cavity surfaces are oxidized. In "secondary" pipe there is no opening to the atmosphere and the cavity surfaces are not oxidized. Secondary pipe can be healed by further hot working, while primary pipe cannot.
   c. *Burst.* An internal void or crack, generally in the center of the bar, due to improper hot-working procedures.
   d. *Center porosity.* Possibly due to a discontinuity, such as pipe, or to gas evolution.
   e. *Nonmetallic inclusions.* Generally concentrated toward the center of the

ingot during solidification. Many inclusions will appear as pits after hot etching.

f. Metallic segregates. Also concentrated toward the center of the ingot during solidification.

g. Internal cracks. Flakes and cooling cracks due to excessive hydrogen content.

h. Dendrites. Results from the solidification process and are present in most cast metals.

i. Pattern effect ("*ingot pattern*"). A result of the solidification characteristics of the ingot and not a cause for concern, unless inclusions have segregated to the pattern interface.

j. Decarburization. Occurs at the surfaces of steel ingots and billets during processing and shows up as a light etching rim.

k. Carburized surfaces. Surfaces that etch darker than the interior of the disc due to enrichment of carbon content.

l. Hardness patterns and soft spots. Revealed by etch contrast.

m. Flow lines. Result from hot working and are revealed on longitudinal samples. The inclusions and segregates elongated by hot working are preferentially attacked by etching.

3. Macroscopic features in continuously cast metals

a. Axial porosity. Porosity exhibited by continuously cast metals (as-cast) along the centerline that is due to incomplete feeding during solidification.

b. Large inclusions. Oxidation of the pouring stream, generally between the tundish and the mold, that produces large oxide inclusions.

c. Segregation streaks. Stressing (mechanical or thermal) of the solidifying steel that produces internal cracks which are immediately filled by metal enriched with sulfur from the interdendritic regions.

d. Segregation bands. Light and dark etching bands that are sometimes observed on transverse sections. These bands are produced by excessive or uneven secondary water spray cooling. They are also referred to as halfway or midway cracks, radial streaks, or ghost lines.

e. Triple-point cracks. Cracks that occur in continuously cast slabs. When observed on a transverse section, they are perpendicular to the narrow side of the slab within the V-shaped region where the three solidification fronts meet. These cracks are caused by bulging of the wide slab face, which results from inadequate containment of the solid shell.

f. Centerline cracks. Cracks that form in the center area of the cast section near the end of solidification. The cracks are caused by bulging of the wide slab face or by a sudden drop in centerline temperature.

g. Diagonal cracks. Cracks that occur in billets as a result of distortion of the billet into a rhomboid section. The distortion may be cause by nonuniform cooling, such as when two adjacent faces cool more rapidly than the other faces.

h. Straightening or bending cracks. Cracks that occur during straightening or bending procedures if the center of the section is still liquid or above 1340°C.

i. Pinch-roll cracks. Cracks that can be caused by excessive roll pressure applied when the center is still liquid or above 1340°C.
j. Longitudinal midface cracks. Surface cracks observed on slabs.
k. Longitudinal corner cracks. Cracks at the corners of billets and blooms that are due to compositional and operating factors.
l. Transverse, midface, and corner cracks. Surface cracks that occur at the base of oscillation marks. Steel composition is a critical factor in their formation.
m. Star cracks. Surface cracks that occur in clusters, each having a starlike appearance. They are generally fairly shallow and are usually caused by copper from the mold walls.

4. Macroetch features of consumable electrode remelted steels
   a. Freckles. Circular or nearly circular dark etching spots due to concentration or carbides or carbide-forming elements.
   b. Radial segregation. Radially or spirally oriented dark etching elongated spots generally located at midradius. These areas are usually enriched with carbides.
   c. Ring pattern. Concentric rings (one or more) which etch differently than the bulk of the disc as a result of minor variations in composition.
   d. White spots. Globular light-etching spots due to a lack of carbide or carbide-forming elements.

1-3 APPLICATIONS OF MACROETCHING

The various imperfections or defects just described can be detected by hot-acid etching. Since the cross section usually provides more information than the longitudinal section, the general practice is to cut discs transversely, i.e., perpendicular to the hot-working axis. To facilitate handling, disc thickness should generally be 1 in or less. Longitudinal sectioning is used to study fiber, segregation, and inclusions.

1-3.1 Solidification Structures

The structure resulting from solidification can be clearly revealed by macroetching. Figure 1-1 shows the macrostructure of a transverse disc cut from a small laboratory-size steel ingot that was etched with 10% HNO_3 in water. At the mold surface, there is a small layer of very fine equiaxed grains. From this outer shell, large columnar grains grow inward toward the central, equiaxed region.

Figure 1-2 shows the macrostructure of a 99.8% aluminum centrifugally cast ingot after a minor degree of reduction. There is a thin band of fine grains around the edge, which is considerably thicker in the area near the left side of the photograph. Rather coarse columnar grains are observed growing from the outer surface, merging at a spot which is off center.

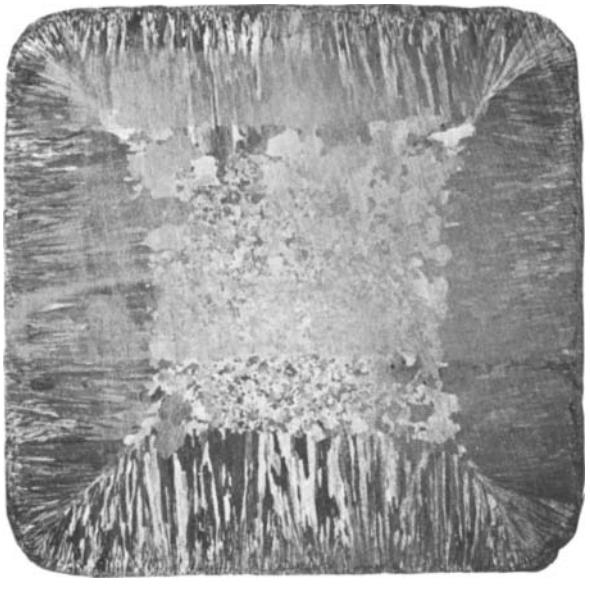

Figure 1-1 Cold etch of disc cut from small ingot (10% aqueous HNO_3).

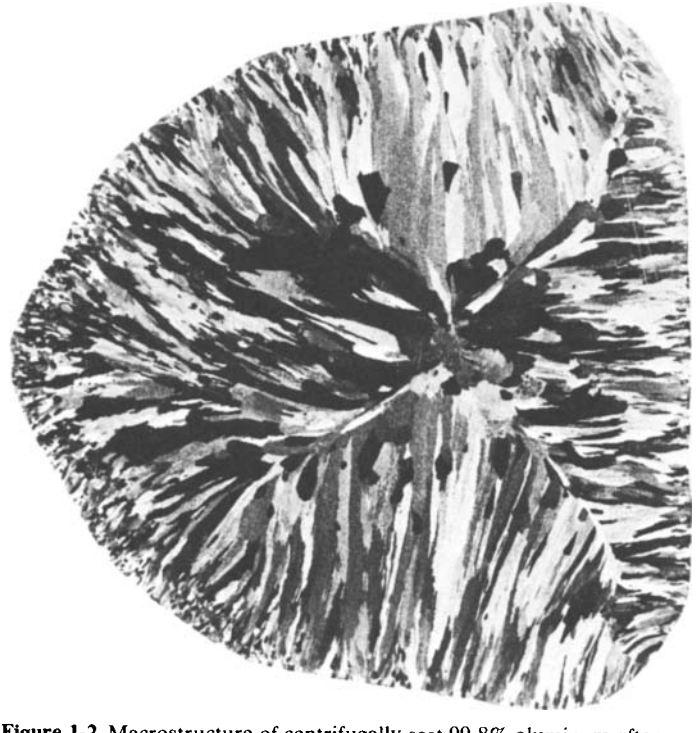

Figure 1-2 Macrostructure of centrifugally cast 99.8% aluminum after a minor amount of reduction (3¼×; etchant, solution of 5 mL HNO_3, 5 mL HCl, 5 mL HF, and 95 mL H_2O). *(Courtesy of R. D. Buchheit, Battelle-Columbus Laboratories.)*

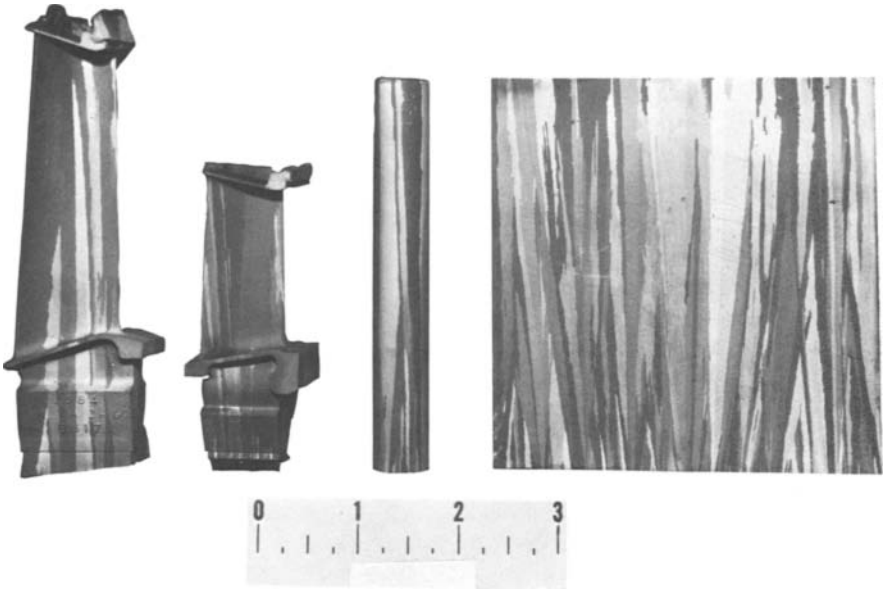

Figure 1-3 Macrostructure of directionally solidified nickel-base eutectic alloy (etchant, solution of 1 mL H_2O_2 and 99 mL HCl). *(Courtesy of W. Yankausas, TRW, Inc.)*

The presence of a coarse columnar grain structure can impart useful properties to a material that is to be used at high temperature. Considerable effort has been made to preferentially grow such grains in high-temperature alloys used in turbines. Figure 1-3 shows the macrostructure of a directionally solidified nickel-base eutectic alloy in several product forms.

1-3.2 Billet and Bloom Macrostructures

In general, the steelmaker uses the hot-acid etch on discs cut, with respect to the ingot location, from the top and bottom or the top, middle, and bottom of billets or blooms† rolled from the first, middle, and last ingots teemed from the heat. If a disc reveals a rejectable condition, billet material is rejected until the condition is removed.

Figure 1-4 shows "dirty" corners, a lap, several small seams, and freckle-type segregation in a hot-acid etched disc of bearing steel. The inclusion present in the dirty corner (lower right) is a Mn-Fe-Al silicate. Figure 1-5 shows ingot pattern and pits from inclusions in alloy steel. In Figure 1-6 the standard hot etching has revealed entrapped gas, heavy segregation, voids, and ingot pattern in a disc of AISI 4140 alloy steel. Figure 1-7 shows the microstructure near the center of this disc (longitudinal plane through the disc). The center of the disc is coarse and exhibits an open pipe condition and associated segregation.

† Blooms are rolled sections larger than 6 by 6 in, while billets are smaller than this.

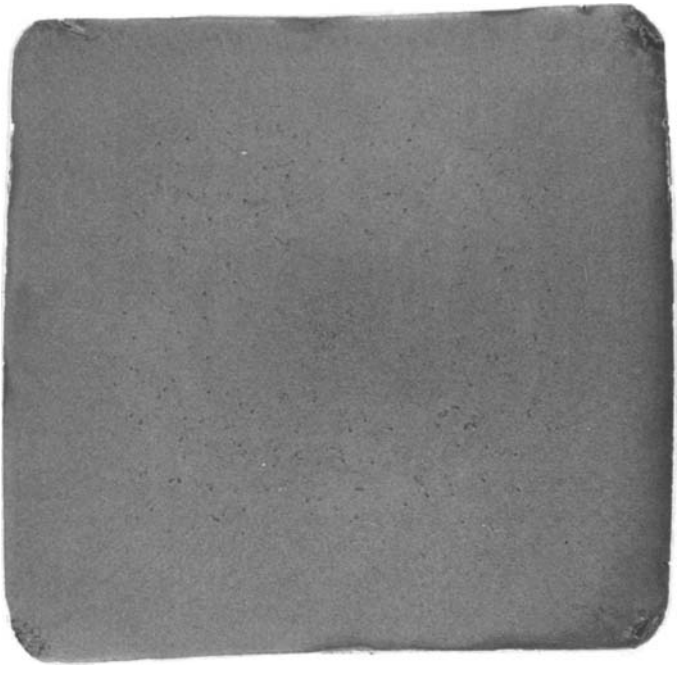

Figure 1-4 Hot-acid etching of this disc from a bearing steel billet revealed broken corners, a lap (upper left), several small seams, and freckle-type segregation.

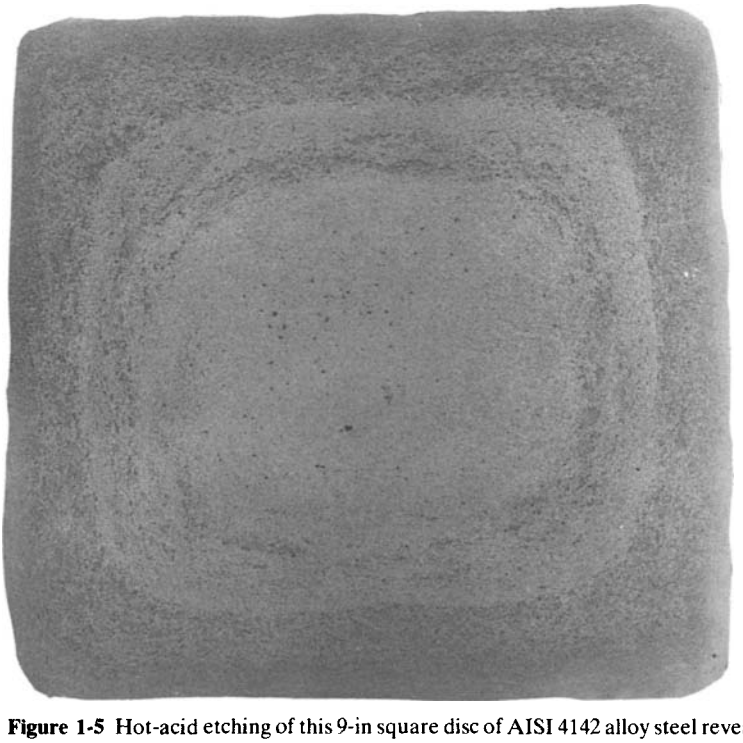

Figure 1-5 Hot-acid etching of this 9-in square disc of AISI 4142 alloy steel revealed ingot pattern and inclusion pits.

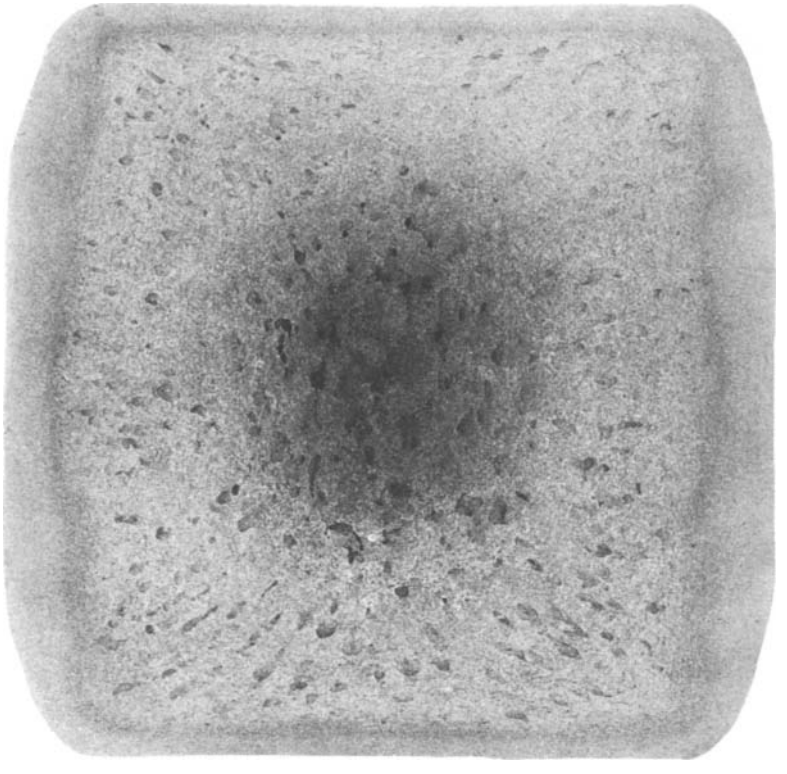

Figure 1-6 Hot-acid etching of this disc from an AISI 4140 alloy steel billet revealed entrapped gas, heavy segregation, voids, and ingot pattern.

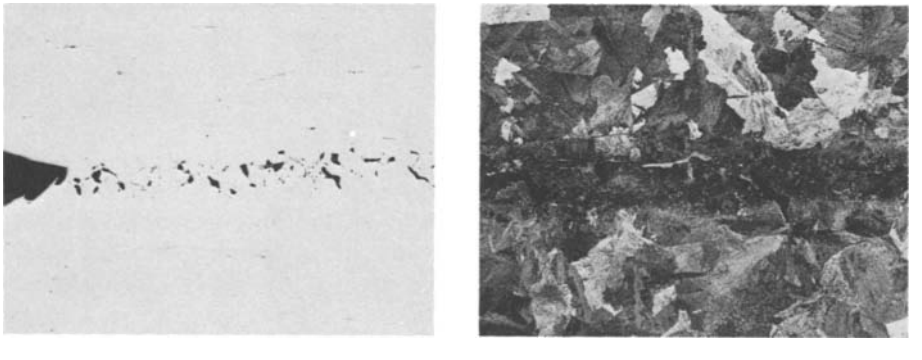

Figure 1-7 Microstructure in central region of etch disc shown in Fig. 1-6 revealing an open pipe condition and segregation (unetched, 25×; etched with 2% nital, 50×).

Figure 1-8 Hot-acid etching of this disc from an AISI 1050 billet revealed a "cokey" center, inclusion pits, and a dendritic pattern.

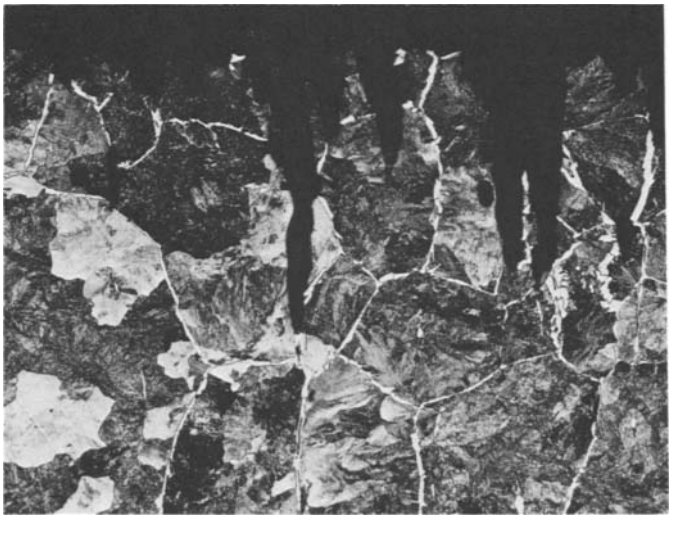

Figure 1-9 Microstructure in "cokey" like center of etch disc shown in Fig. 1-8 revealing the depth of the etch attack (2% nital, 75×).

Figure 1-10 Hot-acid etching of this disc from an AISI 4145 modified alloy steel billet revealed hydrogen flakes.

Figure 1-8 shows a "cokey" center, pits, and a well-defined dendritic pattern in a disc of carbon steel. Figure 1-9 shows the microstructure (longitudinal plane through etched disc) in the "cokey" region. Note the coarse grains outlined by ferrite. Sulfide inclusions that are oriented in the hot-working direction were frequently observed in the ferrite phase. Note that the etch has severely attacked the sulfide stringers, which are more numerous in the "cokey" region.

In Figure 1-10, hydrogen flaking is sharply delineated by standard etching of a disc of alloy steel. Figure 1-11 shows a macroetched disc cut from a Ti-6Al-4V forging. Note the pronounced flow-line pattern around the forging lap.

1-3.3 Continuously Cast Steel Macrostructures

In recent years, continuous casting has become an important process for producing metals. Macroetching has been widely employed in the development of this technique, to evaluate the influence of casting parameters on billet and slab quality and on the quality of the wrought product. Some examples of the unique macroetch features that can be observed in such steels are given in the following examples.

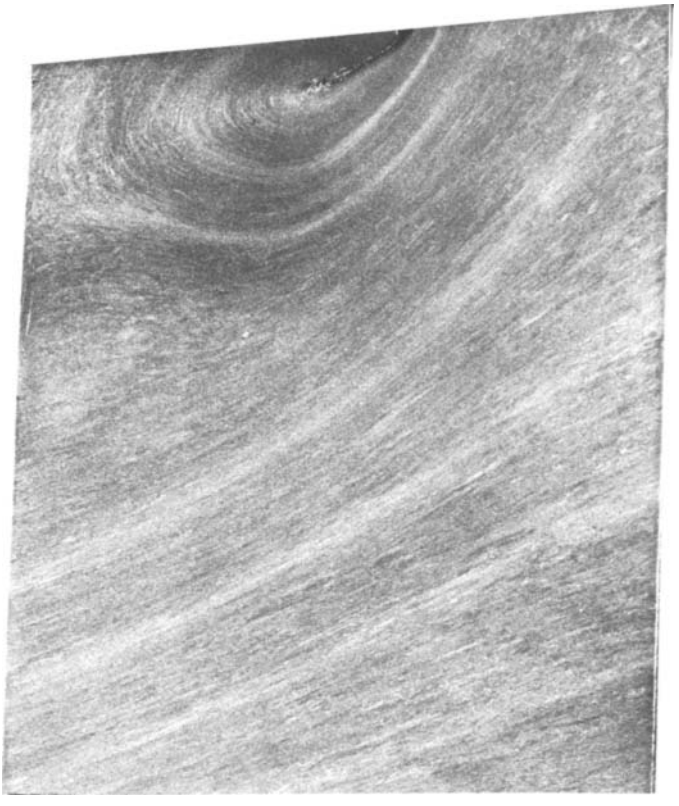

Figure 1-11 Macroetching of a Ti-6Al-4V forging revealed grain flow and a forging lap (1¼×; etchant, solution of 10 mL HF, 15 mL HNO_3, and 75 mL H_2O for 2 min at room temperature). *(Courtesy of J. A. Hendrickson, Wyman-Gordon Co.)*

Figure 1-12 shows the macrostructure of continuously cast carbon steel. Hot-acid etching revealed an unconsolidated center and halfway cracks in the transverse (Fig. 1-12*a*) and longitudinal (Fig. 1-12*b*) discs. Figure 1-13 shows the macrostructure of carbon steel that contained a star-type crack pattern. This crack was not completely healed during rolling. Figure 1-14 shows an etched disc from the transverse section of continuously cast AISI 4140 that revealed a dendritic structure, center porosity, and a light etching band from induction stirring.

1-3.4 Consumable Electrode Remelted Steel Macrostructures

Electroslag-remelted and vacuum-arc-remelted steels can exhibit unique macroetch features. Steels produced using these refining practices have a grain structure with an oriented growth pattern which is essentially vertical but inclined toward the center which eliminates the central equiaxed portion of the ingot with

its high inherent segregation and reduces both macrosegregation and microsegregation.

Figures 1-15 and 1-16 show the macrostructures of billets rolled from electroslag-remelted ingots and illustrate some of the unique features that can be encountered. Figure 1-15 shows an etched disc exhibiting a light freckle condition. Figure 1-16 shows a ring pattern and a few randomly dispersed pits.

1-3.5 Dendrite Arm Spacing

For many years, efforts to improve the properties of castings were directed primarily at refining the grain size. While these efforts definitely produced improvements in mechanical properties, it has since been recognized that other factors must also be controlled. Optimum properties can be achieved through control of the as-cast dendritic structure.

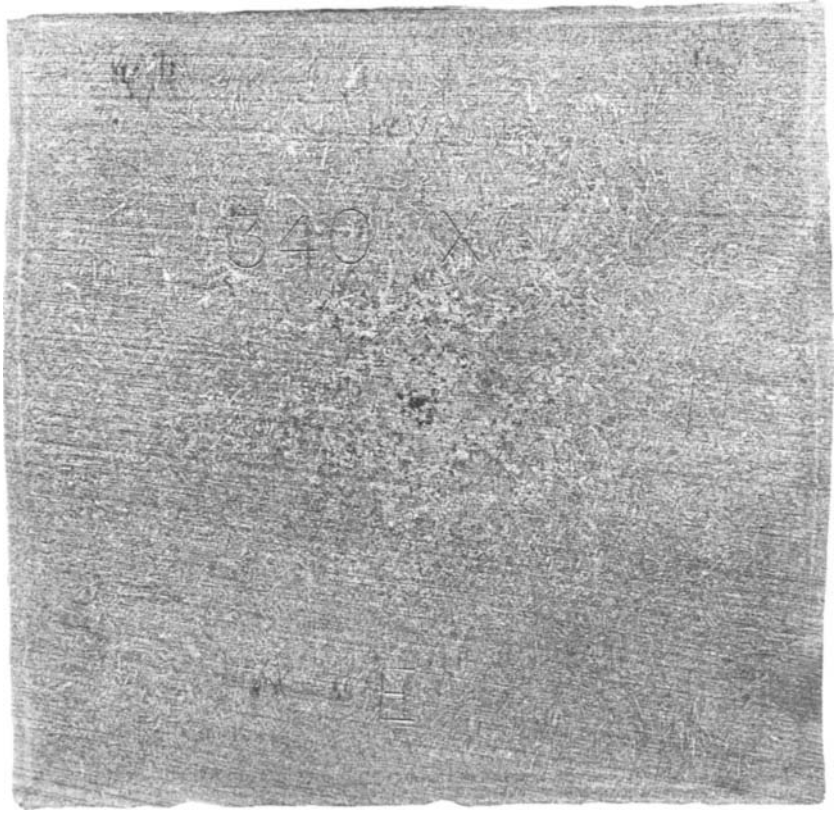

Figure 1-12*a* Hot-acid etching of a transverse disc from continuously cast AISI 1045 carbon steel revealed coarser dendrites at top compared to bottom, light center segregation, and halfway cracks. *(Courtesy of M. Schmidt, Bethlehem Steel Corp.)*

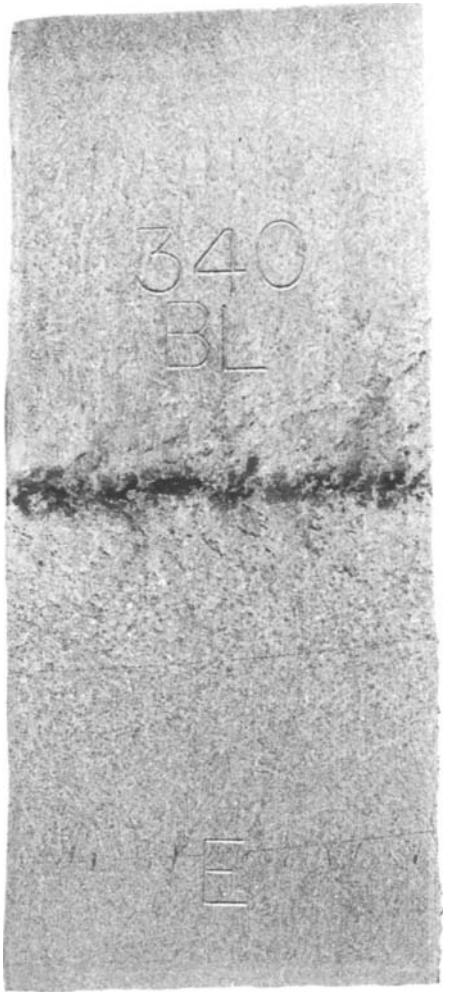

Figure 1-12*b* Hot-acid etching of a longitudinal disc from the center of the disc shown in Fig. 1-12*a* revealed the extent of the open center condition. *(Courtesy of M. Schmidt, Bethlehem Steel Corp.)*

Figure 1-13 *(Top of opposite page)* Hot-acid etching of a transverse disc from continuously cast AISI 1008 carbon steel revealed a star-pattern open condition. *(Courtesy of M. Schmidt, Bethlehem Steel Corp.)*

Figure 1-14 *(Bottom of opposite page)* Hot-acid etching of this transverse section of continuously cast AISI 4140 revealed a dendritic structure, center porosity, and a band (arrow) from induction stirring. *(Courtesy of B. L. Bramfitt, Bethlehem Steel Corp.)*

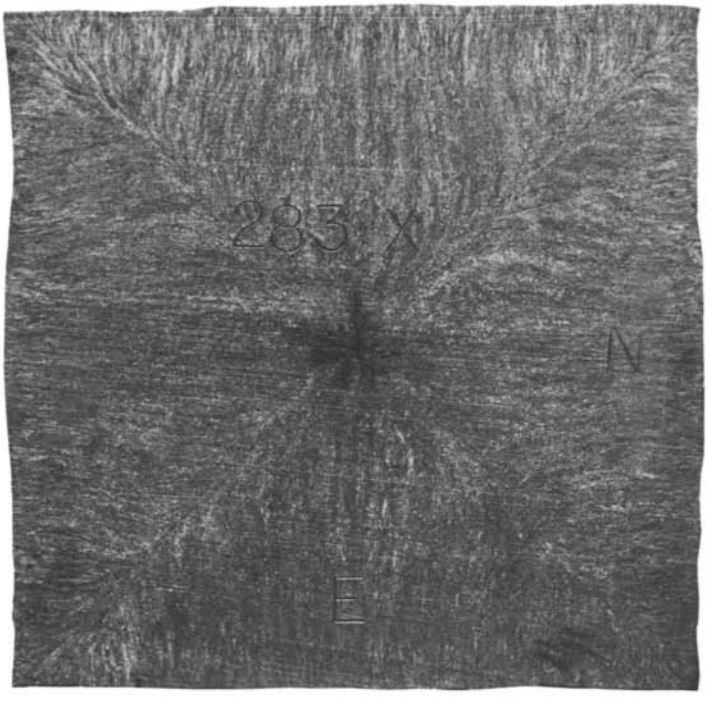

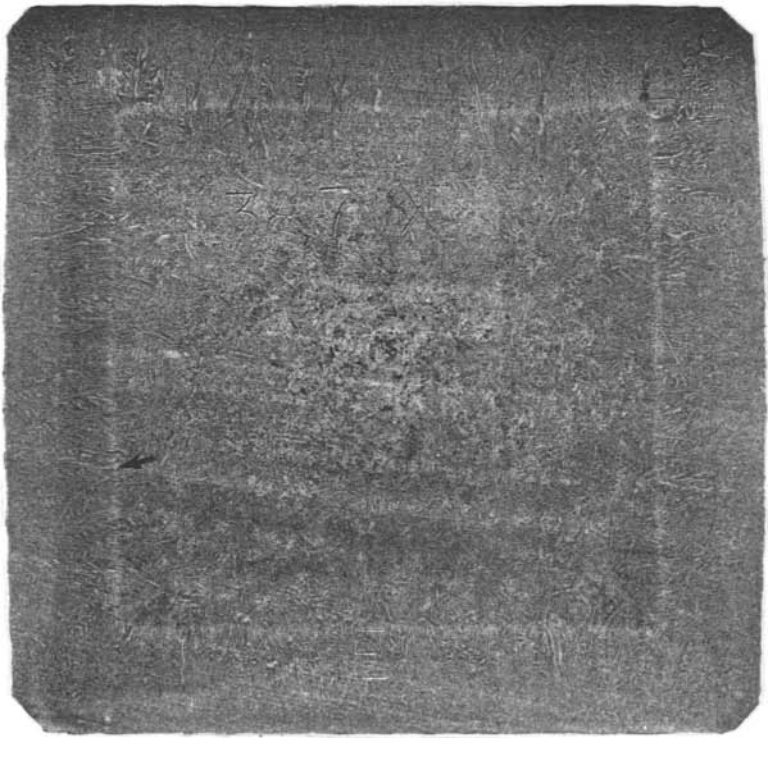

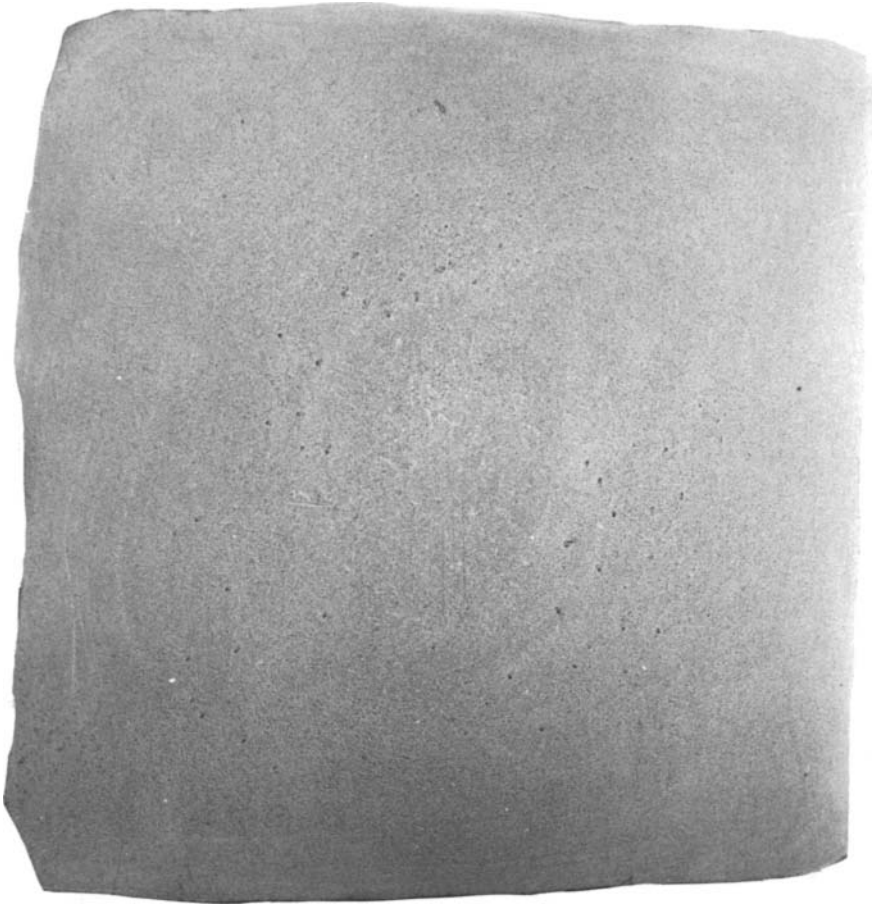

Figure 1-15 Hot-acid etching of this disc from an electroslag-remelted tool steel billet revealed light freckle segregation and a faint, discontinuous ring pattern. *(Courtesy of M. H. Lasonde, Bethlehem Steel Corp.)*

Dendrites grow initially in the form of rods. However, growth perturbations or minor changes in the liquid around the growing dendrite occur. These temperature and compositional perturbations in the liquid cause bumps to form on the side of the rods, which grow outward into the liquid forming the secondary arms. In a like manner, tertiary arms can form on the secondary arms and so forth. Later, the liquid between the primary, secondary, and tertiary arms freezes. The planes containing the primary stalk and a secondary arm are called primary sheets. These planes are parallel to the direction of heat flow. Planes perpendicular to the primary sheets containing secondary and tertiary arms are called secondary planes. In the examination of dendrite structures, low magnifications (10X for example) are much more useful than high magnifications (100X and

Figure 1-16 Hot-acid etching of this disc from an electroslag-remelted tool steel billet revealed a well-developed ring pattern and a few randomly dispersed pits. (*Courtesy of M. H. Lasonde, Bethlehem Steel Corp.*)

higher). Figure 1-17 shows dendrites observed on a broken tensile bar from a casting. The primary and secondary arms are readily visible, and tertiary arms can be detected occasionally.

The primary and secondary arm spacings have been measured in solidification studies. The secondary arm spacing has been shown to be a sensitive measure of solidification phenomena. While most studies have measured the secondary arm spacing, Weinberg and Buhr measured the primary dendrite spacing because it changes more rapidly with freezing distance than the secondary arm spacing [14].

The basic difference between the primary and secondary arm spacings can be viewed in terms of nucleation and growth mechanisms. The primary dendrite stalks develop from grains that nucleate at the chill surface. Only those grains with

9X

Figure 1-17 Dendrites observed on a broken section of cast iron.

the proper crystallographic orientation will grow an appreciable distance into the liquid. In body-centered cubic metals, such as iron, the direction of dendrite growth is always the cube axis, i.e., <100>. The primary dendrite spacing depends upon the initial freezing conditions in the chill zone and thus is controlled by the nucleation rate. However, the secondary arm spacing is not a function of the nucleation rate at the chill surface but is controlled by the growth rate away from the surface. Thus, the critical factor for the secondary arm spacing is the rate of heat removal from the casting. The degree of heat removal changes constantly during most casting processes, and therefore measurement of the secondary arm spacing is of considerable value in the study of solidification. Although some qualitative information regarding dendritic spacing was known, Alexander and Rhines performed the first quantitative study of the solidification process [15]. In this report Alexander and Rhines discussed the problem of making measurements of dendrite spacing. In order to eliminate the need for corrections for orientation effect, they first made spacing measurements only in grains where the major dendrite axis was nearly in the plane of polish. Since this is a matter of judgment, some error can be introduced. They observed that not all of the secondary arms were well developed, and chose to measure only spacings between fully developed secondary arms. Since this is also a matter of judgment, error can result and the degree of repeatability of measurements suffers. They also observed that two characteristic spacings were present in the center of some of their ingots; they chose to record the larger spacing rather than the smaller or an average of the two.

In some metals, such as aluminum castings, it is difficult to measure dendrite arm spacings. In these metals, one can measure the dendrite cell size, which is the width of the individual cells, or the dendrite cell interval, which is the center-to-center distance between adjacent cells. In alloys with a small amount of interden-

dritic material, the cell size and cell interval are equal. However, as the amount of interdendritic matter increases, the cell interval becomes greater than the cell size, and the dendritic cell size is usually the preferred measurement. If the amount of interdendritic material is small, the line intercept method can be used to compute the number of cells per unit length and the average cell size.

1-3.6 Forging Flow Lines

Macroetching is widely used to study metal flow patterns due to hot or cold working. Figure 1-18*a* shows a disc cut from a close-die-forged steering knuckle made from AISI 4140 steel. The disc was deep-etched in the standard hot etch of hydrochloric acid and water. The flow lines can be observed, but they are much

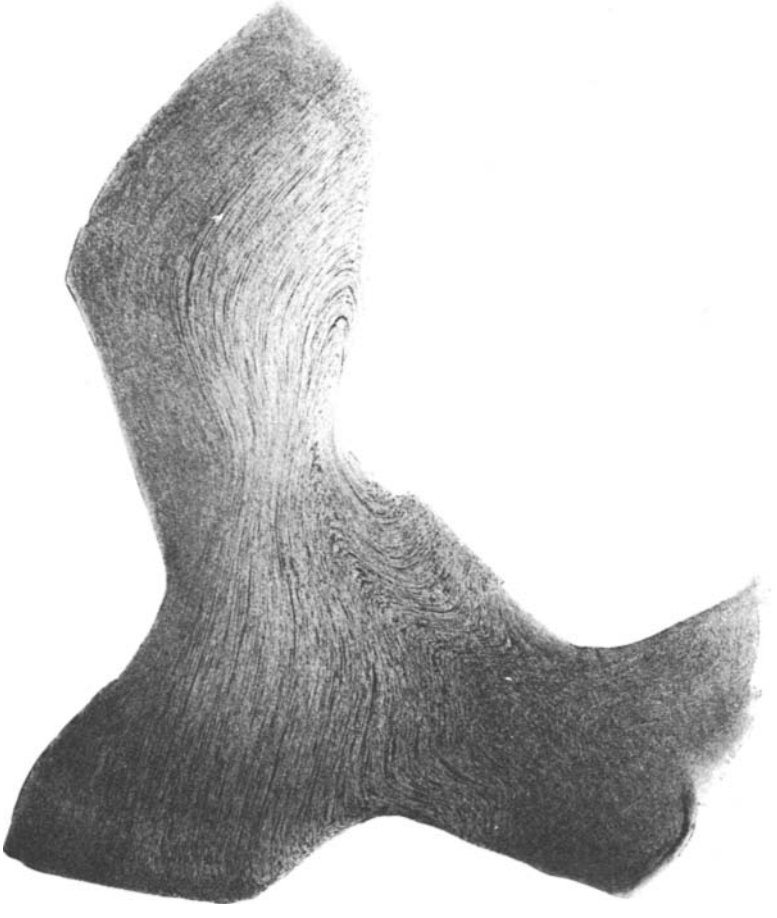

Figure 1-18*a* Flow lines in closed-die-forged AISI 4140 steering knuckle revealed by hot etching with 50% aqueous HCl ($^1/_2\times$).

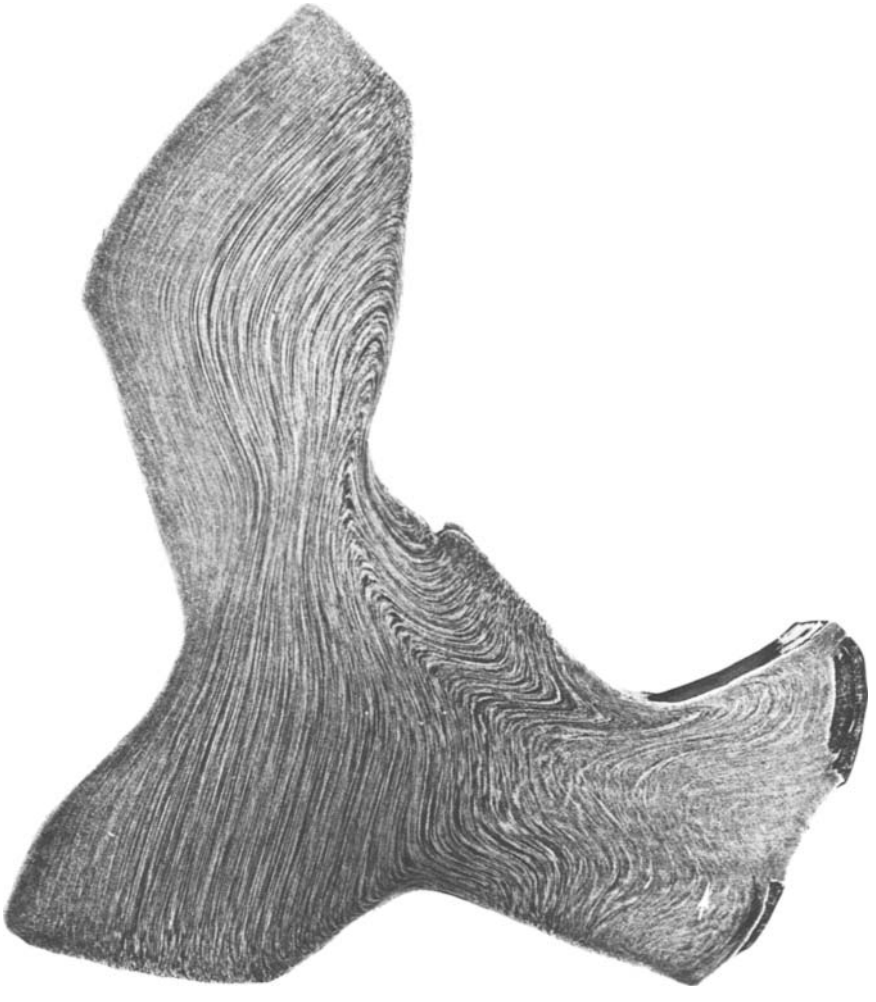

Figure 1-18*b* Flow lines in sample shown in Fig. 1-18*a* that were revealed by deep-acid etching and inking.

more plainly visible after inking, as shown in Figure 1–18*b*. India ink was rubbed over the surface of the component and seeped into the etched-out flow lines; the excess ink was wiped off the top surface.

Figure 1-19*a* shows a disc from a macroetched forging of Ti-6Al-4V; flow lines and segregation can be observed. Figure 1-19*b* shows the microstructure at the four areas. Area A exhibits a uniform alpha-beta structure, while the other three areas exhibit coarse, stringy alpha phase and coarse beta phase.

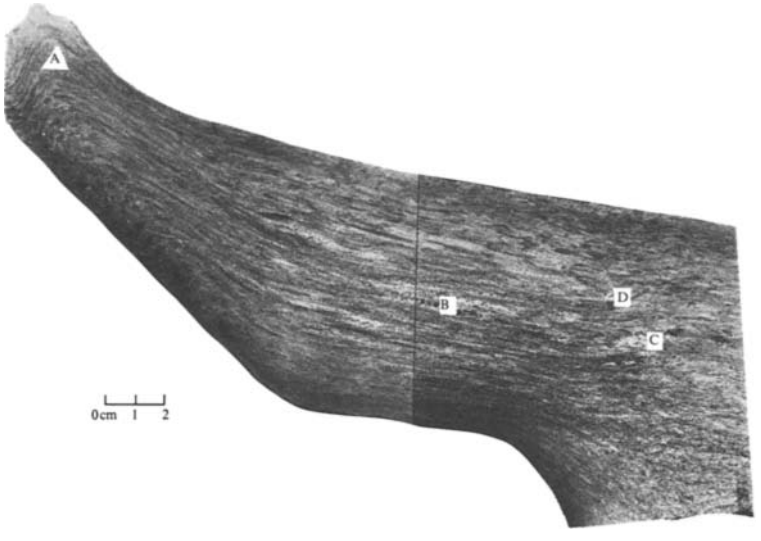

Figure 1-19*a* Macroetching of a section from a Ti-6Al-4V forging revealing metal flow pattern and segregation (etchant, solution of 10 mL HF, 15 mL HNO_3, and 75 mL H_2O, swabbed for 2 min at room temperature). *(Courtesy of J. A. Hendrickson, Wyman-Gordon Co.)*

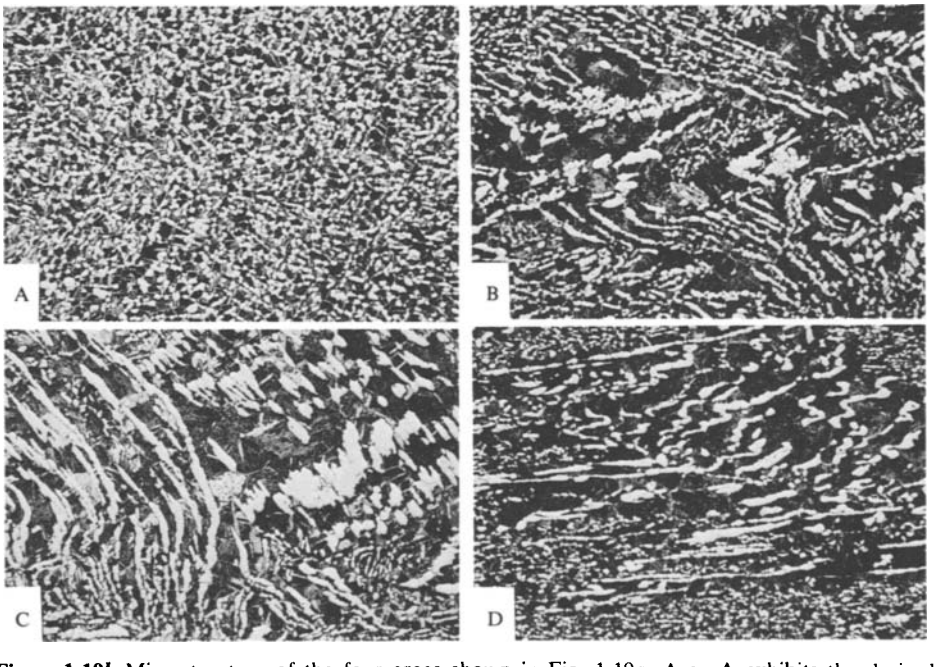

Figure 1-19*b* Microstructure of the four areas shown in Fig. 1-19*a*. Area A exhibits the desired uniform alpha-beta microstructure. Areas B, C, and D show regions of coarse, linear alpha (white) and course beta (dark) phase (60×; 10 seconds immersed with heavy agitation in 8 g NaOH in 60 mL water, heated to a boil after addition of 10 mL H_2O_2). *(Courtesy of J. A. Hendrickson, Wyman-Gordon Co.)*

1-3.7 Grain or Cell Size

As shown in some of the previous examples, macroetching usually reveals the as-cast grain structure, particularly when it is relatively coarse. Figure 1-20 shows a sample of AISI 1020 semikilled steel used as the handle of a basket in a continuous annealing furnace. The surface of the part was heavily decarburized during use, resulting in a coarse columnar grain structure in the decarburized layer. These grains are clearly revealed by etching. The interior, fine-grained structure exhibits a dull mat appearance.

In cast eutectic alloys, the eutectic cell size and the morphology of the eutectic are of the most interest. In hypoeutectic gray cast iron, solidification begins with the formation of austenite dendrites that grow as the temperature falls to the eutectic temperature. At the eutectic temperature, the liquid solidifies as a result of freezing of the eutectic of austenite and graphite. Usually the pattern of eutectic growth roughly approximates a sphere. Growth of the eutectic nuclei continues until they impinge on one another, producing a characteristic cell size which depends on the nucleation rate. Many of the copper-containing reagents (see App. B) can be used to reveal the eutectic cell size and Stead's reagent has been widely used. Eutectic cell size can also be measured by the intercept method. Studies have shown how processing influences cell size and how cell size influences properties.

The eutectic cell boundary exhibits a light etching appearance as a result of the entrapment of impurities, such as phosphorus and sulfur, at the interface. The eutectic cells are most easily viewed with the unaided eye or with low magnifications. In white cast iron, which freezes with an austenite-carbide eutectic, the eutectic cell boundaries can be faintly seen in columnar castings but not in equiaxed castings. In gray irons, there is no relationship between graphite flake size and the eutectic cell size. The eutectic cell size in nodular iron is much

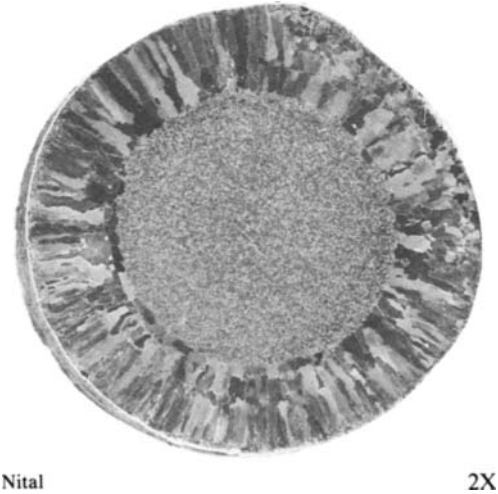

Nital 2X

Figure 1-20 Macroetching of a section cut from an AISI 1020 (semikilled) basket handle used in a continuous annealing furnace revealed coarse dendritic grain growth associated with decarburization.

finer than in gray iron; the finer cell size and the nodular graphite shape account for the remarkable properties of nodular iron.

Delineation of the eutectic cells in gray iron depends on either the segregation or the depletion of certain elements in the cell boundaries. A wide variety of techniques have been used to reveal the eutectic cells. Dawson and Oldfield [16] recommend the following:

1. 4% picral for 5 min—for ferritic type D gray iron
2. Stead's reagent for up to 1 h—good for low-phosphorus pearlitic irons
3. 10% aqueous ammonium persulfate for up to a few minutes—good for high-phosphorus (more than 0.2%) irons

Adams [17] recommends the following:

1. Heat tinting—especially useful for high-phosphorus irons
2. Deep etching in 25% alcoholic nitric acid—good for some high-phosphorus irons
3. Heating samples for 30 to 120 min at about 1300°F (704°C), then polishing and etching them with nital or picral—widely applicable method

Merchant has reviewed many of the methods used to reveal eutectic cells [18].

Eutectic cells can be easily revealed in pearlitic gray iron by heating the specimen below the critical temperature, for example, at about 1300°F (704°C), for 30 min to 2 h [17]. This procedure decomposes the pearlite in the center of the cells, while the pearlite at the cell boundaries is relatively unaffected because the phosphorus at the cell boundaries retards graphitization. With ferritic gray irons or gray irons that are almost or completely ferrite, the sample can be heated [19] to 1800°F (982°C), quenched into lead or salt at 1200°F (649°C), and held there for about 30 s before being quenched with water. This procedure produces a thin film of pearlite at the cell boundaries, while the cell interior is martensite plus some ferrite.

Merchant has studied the influence of composition on eutectic cell delineation [20]. He states that eutectic cell boundaries may be impossible to delineate if the sulfur level is below 0.01%. In the presence of appreciable manganese, addition of titanium improves eutectic cell delineation markedly. However, if the manganese content is low, addition of titanium desulfurizes the melt and reduces a procedure's ability to reveal the cell boundaries. The presence of phosphorus in cast iron does not ensure delineation of the eutectic cells. Carbide-stabilizing elements, such as Cr, Mo, or V, aid the delineation of eutectic cells. Elements such as Bi or Pb also help improve cell delineation.

Dawson and Oldfield [16] state that cell structures can be very difficult to reveal in certain samples, such as heavy sections of cast irons that contain medium to high phosphorus. Very large castings, such as ingot molds, are also difficult to etch for determining eutectic cell size.

While the grains in coarse-grained aluminum castings and wrought products can be revealed by many of the macroetchants listed in App. A, a number of investigators have employed color illumination to improve the grain contrast. Beck has used two etchants, listed in App. A, for revealing grains in aluminum [21, 22]. Illumination was provided by three universal microscope lamps angled to provide oblique light from three directions. Each lamp was fitted with a different color filter to increase the contrast of the reflections from adjacent grains. The sample could be rotated while it was examined at low (10 to 20X) magnification. The sample was kept rotating while the projected image was traced on a plastic sheet so that all the grain boundaries could be sketched.

Ryvola has also shown the value of color filters for improving grain contrast in macroetched aluminum samples [23]. Two illuminators, one with a red filter and the other with a green filter, were placed on opposite sides of the sample to cast oblique light. A blue filter was inserted between the sample and the objective of a stereomicroscope. Rotation of the sample was also used here to reveal all the grain boundaries. In most studies Ryvola employed Tucker's or Poulton's reagent (see App. A for composition) as the macroetch.

1-3.8 Alloy Segregation

Because most engineering alloys freeze over a range of temperatures and liquid compositions, the various elements in the alloy segregate during the solidification of ingots and castings. Segregation occurs over short distances, causing microsegregation, and over long distances, producing macrosegregation. Microsegregation is a natural result of dendritic solidification because the dendrites are purer in composition than the interdendritic matter. Macrosegregation manifests itself in a variety of forms–centerline segregation, negative cone of segregation, A- and V-type segregates, and banding. These phenomena are the result of the flow of solute-enriched interdendritic liquid in the mushy zone during solidification; this flow is a result of solidification shrinkage and gravitational forces.

Macrosegregation can be detected by bulk chemical analysis. Tests on large ingots generally reveal low concentrations of carbon and alloying elements at the bottom and sides and enrichment at the top and along the centerline. Macrosegregation can be detected on fractures and on macroetched discs. In addition to the use of traditional macroetching and microetching, microsegregation has also been studied by autoradiography, microradiography, electron-probe microanalysis, and x-ray fluorescence. The study of segregation has become a relatively simple matter since the development of the electron microprobe. This instrument is capable of providing accurate, rapid determinations of compositional differences.

Figure 1-21 illustrates the use of macroetching to reveal segregation and shows a sample of carbon-manganese-chromium steel which cracked during extrusion (note the central burst). A transverse disc reveals a spot of segregation which is more readily observed on the longitudinal section. The streaks are martensitic with a hardness of 46 to 58 HRC (Rockwell hardness on the C scale), while the bulk hardness is below 20 HRC. The streak is enriched in C, Mn, and Cr.

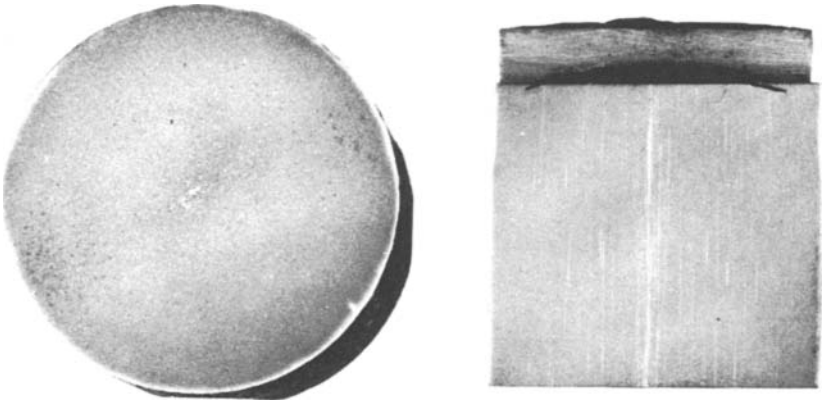

Figure 1-21 Examples of segregation associated with central bursts in extruded AISI 1141 modified steel. The streaks, which consist of martensite, have a hardness of 46 to 58 HRC (Rockwell hardness on the C scale) while the matrix hardness is less than 20 HRC.

1-3.9 Carbide Segregation

Macroetching is also widely used with high-alloy steels to reveal carbide segregation. Figure 1-22 shows longitudinal sections of T1 high-speed steel that have been polished and etched, revealing carbide segregation.

1-3.10 Weldments

Welding has become one of the most important fabrication processes for a variety of reasons. In any study of welds, the initial step invariably centers on the development of the weld macrostructure. The weld macrostructure is established

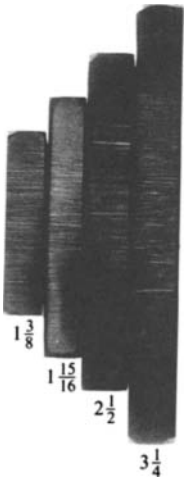

Figure 1-22 Macroetching with 10% nital was used to reveal carbide segregation in polished sections from various sizes of rounds of T1 high-speed tool steel. (Diameters in inches below sections.)

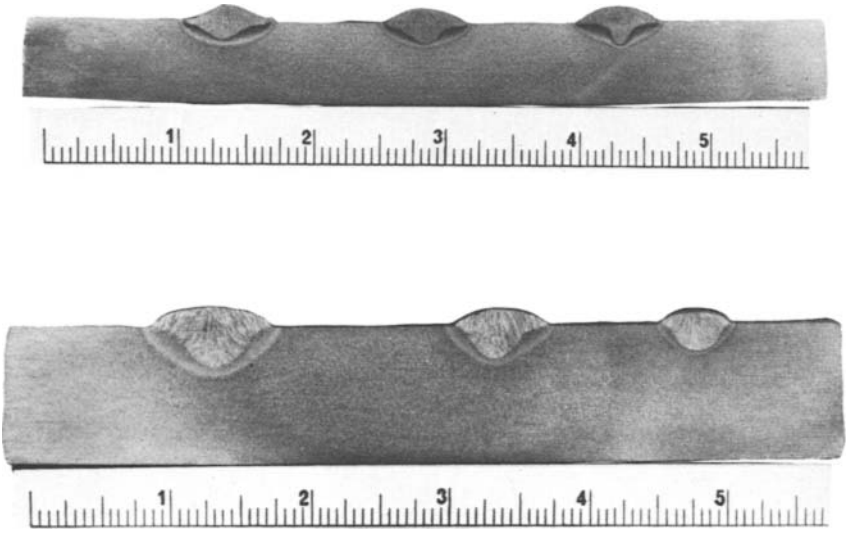

Figure 1-23 Macroetching used to reveal the influence of weld parameters on penetration depth and shape. Top example shows GMA (gas-metal arc) welds at a heat input of 45 kJ/in using atmospheres of 100% CO_2, argon plus 25% CO_2, and argon plus 2% O_2 (left to right). Bottom example shows submerged arc welds using heat inputs of 90, 60, and 30 kJ/in (left to right). (The etchant was 10% aqueous HNO_3.)

by the type of process employed, the operating parameters, and the materials used. Thus, metallography is a key tool in weld quality studies. Key terms in describing the macrostructure of fusion welds are the basic three components—the weld metal ("nugget"), the heat-affected zone (HAZ), and the base metal. Within the weld metal and the heat-affected zone, there are changes in composition, grain size and orientation, microstructure, and hardness. Thus one observes significant variations in microstructure as the weldment is scanned.

Macroetching is frequently employed to determine the influence of various changes in weld parameters on the size and shape of the weld metal, on depth of penetration, on weld structure, and on hardness. Figure 1-23 (top) shows the influence of the protective atmosphere on the shape and penetration of the weld metal. A carbon-manganese plate steel was welded using the gas-metal arc (GMA) procedure with a heat input of 45 kJ/in and 0.045-in diameter A675 filler metal wire. Three atmospheres were used: 100% CO_2 (left), argon plus 25% CO_2 (center), and argon plus 2% O_2 (right). Also shown in Fig. 1-23 (bottom) are three submerged arc weldments that were made using heat inputs of 90 (left), 60 (center), and 30 kJ/in (right). These examples clearly show how welding parameters can alter the size, shape, and penetration of the weldment.

Figure 1-24 illustrates the macrostructure of a weld in beryllium. This sample was polished and the macrostructure was revealed using crossed polarized light. Figure 1-25 shows the macrostructure of flash-welded titanium after etching.

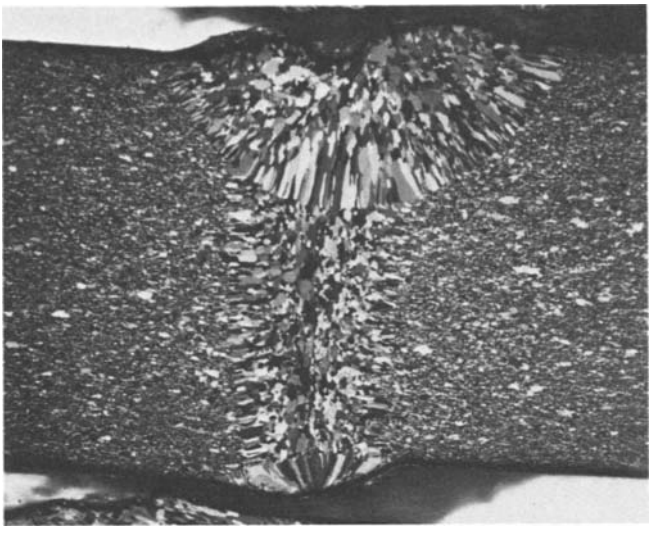

Figure 1-24 Crossed polarized light was used to reveal the macrostructure of this beryllium weldment. *(Courtesy of R. D. Buchheit, Battelle-Columbus Laboratories.)*

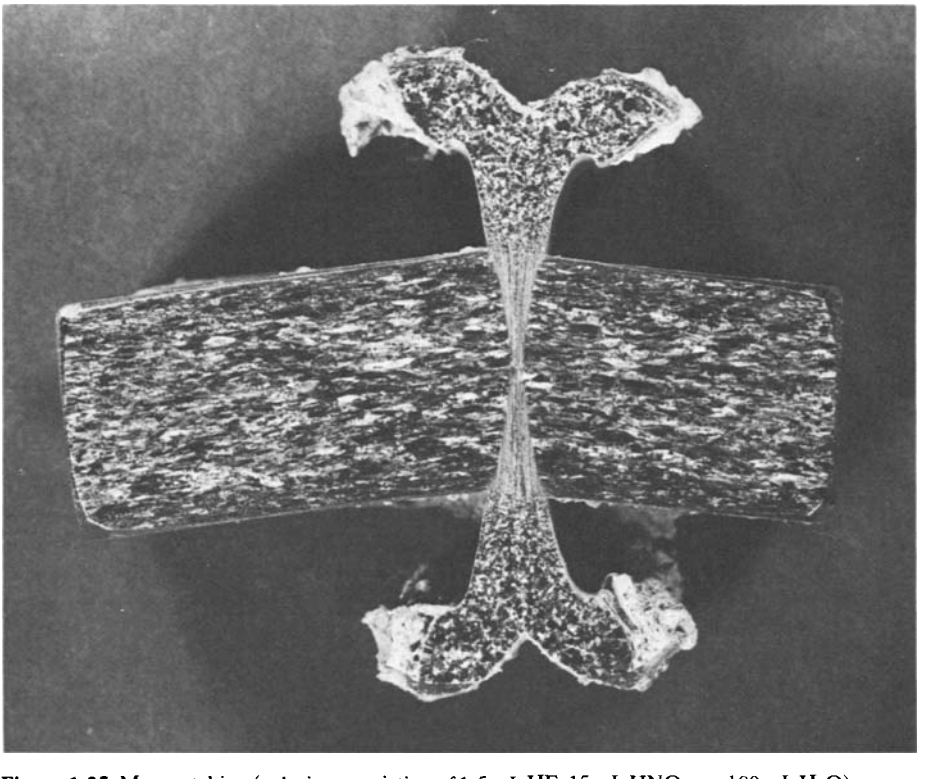

Figure 1-25 Macroetching (solution consisting of 1.5 mL HF, 15 mL HNO_3, and 80 mL H_2O) was used to reveal the macrostructure of this titanium flash weld. The extent of the metal extruded from the joint and the grain refinement in the junction is clearly revealed. *(Courtesy of R. D. Buchheit, Battelle-Columbus Laboratories.)*

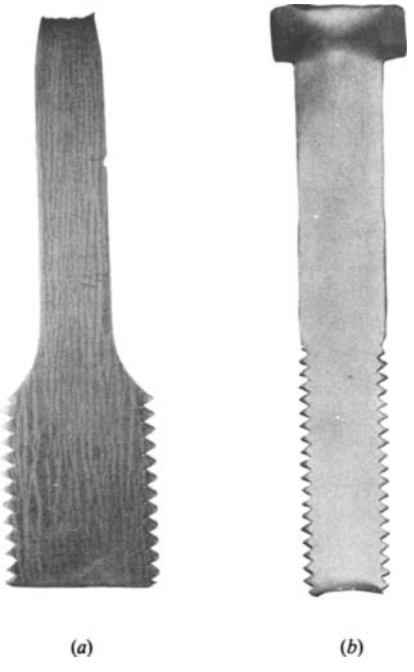

Figure 1-26*a* Strain pattern revealed in a broken flat tensile bar of carbon steel using Bish's procedure (see Refs. 11 and 12).

Figure 1-26*b* Strain pattern in a cold-formed ASTM A325 high-strength bolt (before heat treatment) revealed by Bish's method (see Refs. 11 and 12). Note the thin strained surface layer beneath the cold-rolled threads.

1-3.11 Strain Patterns

As described previously, a number of etching procedures have been developed to reveal strain pattens in steel (App. B) and in aluminum and nickel-base alloys (App. C). Most of these procedures are qualitative in nature. However, Benson has calibrated etching response for residual stresses in AISI 4340, D6AC, and AISI 1045 steels [24]. Etching of the steel revealed regions of tensile elastic surface stresses, forming furrows aligned roughly perpendicular to the tensile stress direction. The furrow spacing was found to vary with the stress level.

The use of etching procedures to reveal strain patterns is illustrated in Figs. 1-26*a* and *b*. The left macrograph (Fig. 1-26*a*) shows the strain pattern observed in a flat tensile test specimen of a light-gauge plate steel, while the right macrograph (Fig 1-26*b*) shows the strain pattern in a cold-formed ASTM A325 bolt.

1-3.12 Failure Analysis

Macroetching can be a useful procedure for the failure analyst [25], as shown by the following examples. Cold etching reveals decarburized surfaces. Figure 1-27 shows a disc cut transversely from a heat-treated steel bar that was cold-etched with 10% nitric acid in water to reveal a light etching rim of decarburization.

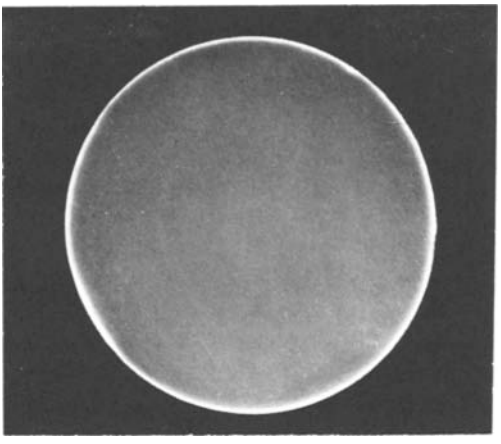

Figure 1-27 Macroetching with 10% aqueous HNO_3 was used to reveal the decarburized surface on this bar (¾×).

Figure 1-28 shows a disc cold-etched with 10% aqueous nitric acid that had been cut from a cracked 3½-in diameter AISI H11 pump plunger. Cracking was detected during finish grinding. Since microscopic examinations showed that both the crack wall and OD (outside diameter) surface were nitrided, cracking occurred prior to nitriding.

Figure 1-29 shows a section that was cut from a carburized AISI P2 die. The etch pattern is characteristic of a carburized steel sample where the case is hard [65 HRC (Rockwell hardness on the C scale)] and the core is unhardened [85 to 86

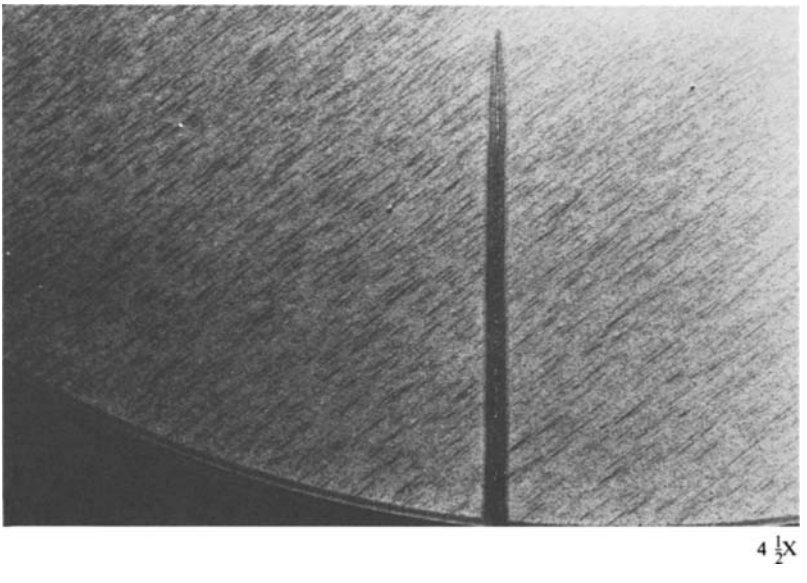

Figure 1-28 Macroetching of a disc cut from a cracked AISI H11 pump plunger revealed a dark rim around both the surface and the crack. This rim indicates the depth of the nitrided surface layer and showed that the crack was present before nitriding.

Figure 1-29 Macroetching (10% aqueous HNO_3) of a disc cut from this carburized AISI P2 part revealed a heavy case at both the ID and OD. The surface was 65.5 HRC (Rockwell hardness on the C scale) while the center was at 85 to 86 HRB (Rockwell hardness on the B scale).

HRB (Rockwell hardness on the B scale)]. Note that the high-carbon hardened case etches with a dark coloration, while the unhardened core appears light.

Parts subjected to abusive grinding have a characteristic scorch pattern when cold-etched. Figure 1-30 shows an AISI D2 die that cracked because of thermal stresses from grinding in the as-quenched (untempered) condition.

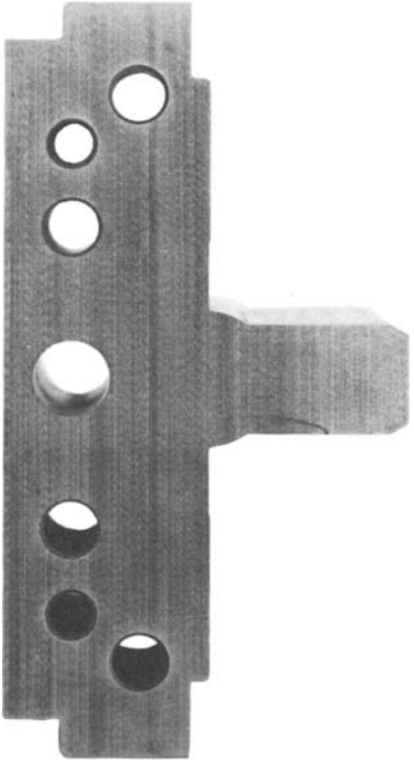

Figure 1-30 Macroetching (10% aqueous HNO_3) was used to reveal grinding scorch on the surface of this AISI D2 die. Grinding damage resulted because the die had not been tempered.

	Bar diameter, in				
	$2\frac{1}{2}$	2	$1\frac{1}{2}$	1	$\frac{3}{4}$
	Hardness, HRC				
Surface	$\frac{60}{61}$	$\frac{60}{60.5}$	$\frac{61}{62}$	62	62
Center	35	32.5	38	58	61.5

Figure 1-31 Macroetching (10% aqueous HNO_3) was used to reveal the extent of hardening in these AISI 1060 carbon steel round bars.

1-3.13 Response to Heat Treatment

Macroetching can also be used to determine the hardenability of various steel bars subjected to known heat treatment conditions. This procedure, coupled with hardness testing, was widely used prior to the adoption of hardenability analysis. As an illustration, Fig. 1-31 shows discs cut from round bars of AISI 1060 carbon steel ranging in size from a diameter of ¾ to 2½ in. The two smallest sizes were through-hardened, that is, the center region contains more than 50% martensite, and the etch pattern was uniform. The other three sizes exhibit a case and core pattern, since the central region was unhardened. For this test, all bars were austenitized at 1525°F (829°C), brine quenched, and then tempered at 300°F (149°C). The bar length was twice the diameter, and the etched section was taken from the center.

Cold etching is also useful in studying the results of surface-hardening treatments. Figure 1-32 shows the results of induction hardening of gear teeth made from AISI 1055 carbon steel. The areas hardened and the depth of the hardened zone are quite apparent.

1-3.14 Flame Cutting

Figure 1-33 illustrates the use of the cold etch to reveal the extent of the heat-affected zone developed during flame cutting of two AISI S5 gripping cams. The etched discs clearly show the effect of different heat inputs on the depth of the heat-affected zone.

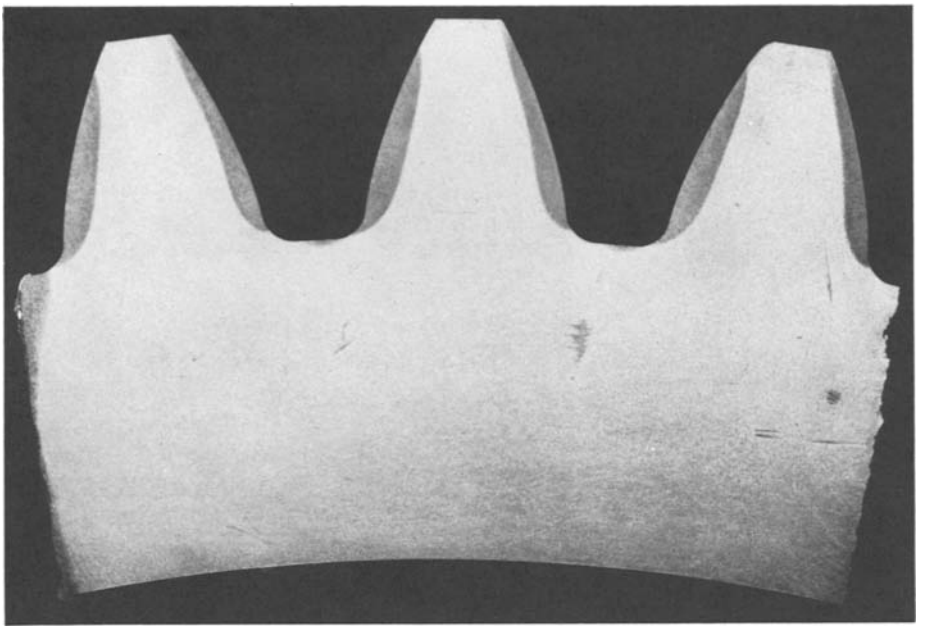

Figure 1-32 The depth and extent of hardening in these induction-hardened gear teeth made of AISI 1055 carbon steel was determined by macroetching with 10% aqueous HNO_3. Surface hardness was 53 to 54 HRC (Rockwell hardness on the C scale), while the unhardened area was about 23 HRC.

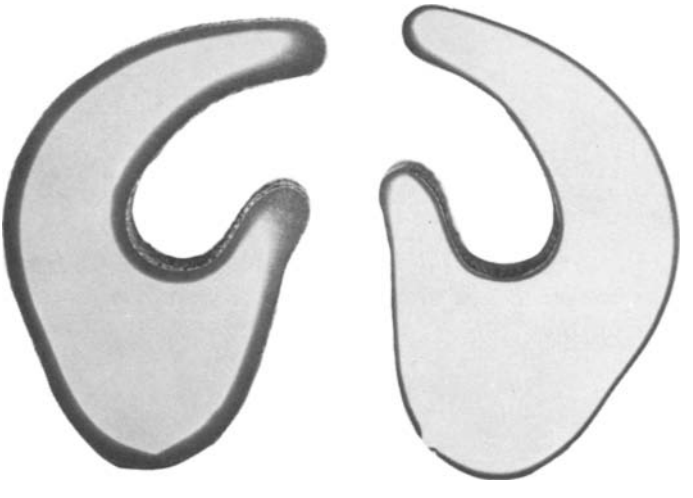

Figure 1-33 Macroetching (10% HNO_3 in water) was used to reveal the extent of the heat-affected zone produced during flame cutting of these AISI S5 tool-steel gripping cams.

1-4 MACROSTRUCTURE REVEALED BY MACHINING

The macrostructure of certain metals and alloys can be revealed by machining. This was first shown by Dewrance in 1927, but no details were provided. Subsequently, Ljunggren showed that the grain structure of soft iron was revealed when the surface was scribed with closely spaced ruled lines just as if it had been etched [26]. Ljunggren also showed that the macrostructure of relatively pure lead was revealed by planing with a microtome. Best results were obtained with the knife blade inclined at an angle of about 4.5° (see Fig. 109, Ref. 26).

Clarebrough and Ogilvie used machining to study the macrostructure of pure lead [27]. The samples were annealed to produce an average grain size of about 5 mm. Orthogonal cuts were made with a high-speed steel microtome with a depth of cut of 0.001 in. Examination of the cut surfaces revealed transverse marks extending across some grains in a direction perpendicular to that of the cut. Grain boundaries were revealed by a change in pitch of these marks. Maximum contrast was obtained when a grain with strong markings was adjacent to a grain without marks. Etch pit techniques, which were used to determine the orientations of grains with strong markings and those without marks, showed that grains with a [100] direction close to the direction of machining formed strong surface marks while grains with a [111] direction close to the direction of machining did not produce marks.

Hanson and Pell-Walpole state that the machining method is the best method for revealing the macrostructure of cast bronzes [28]. They recommend using a sharp, square tool 0.01 in across at the tip, with a depth of cut of 0.01 in and a feed of 0.01 inch.

1-5 THE FRACTURE TEST

Examination of test sample fractures is a well recognized, simple test for evaluating the quality of metals. Indeed, such tests have been conducted since the production of metals first began. In this section, the use of macroscopic examination of sample fractures to evaluate the macrostructure and microstructure of quality control specimens is reviewed.

The breaking of test pieces for examination can be a very crude operation, or it can be carefully controlled in test machines. The simplest procedure is to support the sample on its ends and strike the center with a sledgehammer. In the fracturing of hardened steel discs, a mold can be designed to support the specimen edges, while a top cover is used to locate a chisel over the center of the specimen. The chisel is struck with a sledgehammer to make the break. The mold prevents the broken pieces from striking personnel in the area. If the fracture is desired at a particular spot, it is useful to nick the specimen at the desired spot, and a fracture press is a very useful tool for such work. One end of a specimen can also be placed in a sturdy vise and the specimen struck on the other end. Body-centered cubic metals are occasionally refrigerated in dry ice or liquid nitrogen to facilitate

breaking. Face-centered cubic metals can be difficult to fracture by these methods, especially if the section thickness is appreciable.

Some of the uses of fracture examination include:

- Identification of specimen composition
- Detection of inclusion stringers
- Detection of degree of graphitization
- Assessment of grain size
- Assessment of depth of hardening
- Detection of overheating
- Evaluation of quality

These items are discussed in the sections that follow. A general review of some of these topics is provided in the book by Enos [29].

1-5.1 Composition

In the identification of unknown metals in the field [30], fracture examination can provide a clue to the identity of the material. Along with other visual features, such as color and apparent density, the fracture appearance can be used to provide a rough separation of metals. Ostrofsky provides the following guidelines for use with iron-base alloys [30]:

Metal	Fracture appearance
Gray cast iron	Coarse grain, gray
Malleable iron	Fine grain, black
Wrought iron	Fibrous, light gray
Low-carbon steel	Fine grain, light gray
Tool steel	Very fine grain (silky), light gray

Prior to the development of rapid chemical analysis procedures, the steel melter followed the progress of the refining process by fracture examination. A small sample was poured and cooled rapidly. The sample was broken, and the fracture "read." Obviously, some experience was required. The approximate carbon content was assessed by the degree of brittleness or toughness of the fracture. High oxygen content could be detected by observation of blowholes in the specimen.

1-5.2 Inclusion Stringers

Inclusion stringers of macroscopic size can be readily detected on a fractured specimen after heat tinting in the blue heat range. This procedure is described in

Figure 1-34 Macrograph of a hardened, fractured, and blued macroetched disc revealing inclusion stringers (white streaks).

ASTM Specification E45. There are ASTM specifications that provide fracture test limitations for acceptance for a number of specific materials. Figure 1-34 shows an example of inclusion stringers revealed by use of this procedure.

In most cases where the test is applied, the macroetch discs from the ingots tested are hardened, fractured, and blued on a hot plate or in a laboratory furnace. In general, heating to 500 to 700°F (260 to 371°C) is adequate, although slightly higher temperatures may be required for high-chromium grades. The fracture is always broken so that the fracture plane is longitudinal. The ASTM specifications describe both qualitative and quantitative methods for assessment of inclusion severity. The qualitative assessment can be conducted by comparing the samples to the ten standards in ISO Specification 3763 and noting the distribution of the stringers (core, surface, or uniform). Quantitative assessment requires measuring the length and/or thickness and counting the number in each size range.

1-5.3 Degree of Graphitization

Chill and wedge tests have both been widely employed in the manufacture of gray and white irons to reveal the carbide stability, or the tendency of an iron to solidify as white iron rather than gray iron. These tests show the combined effect of melting practice and composition on carbide stability but are not a substitute for chemical analyses.

Figure 1-35 Fractograph of wedge test specimen of cast iron. The white areas indicate the presence of iron carbide, while the dark areas indicate that flake graphite is present.

Each test uses a different procedure to cast the sample. The chill test uses a small rectangular casting where one face is a chill plate, while the wedge test employs a wedge-shaped casting. In the wedge test, the cooling rate varies with the wedge thickness, and chill plates are not used in the wedge test mold.

After casting a specimen with either method, the sample is broken and the fracture is examined (see Fig. 1-35). In the chill test, the depth of the chill (white iron) is measured. The appearance of the zone between the fully white and fully gray fractures plus the chill depth is an indicator of melting conditions. In the wedge test, the distance from the wedge tip to the end of the white fracture is measured, usually to the nearest $\frac{1}{32}$ of an inch.

In the production of tool steels, the fracture test may be used to detect graphite in tool steels that intentionally incorporate graphite or in high-carbon tool steels that should be free of graphite. Figure 1-36 shows four fractured test discs of a high-carbon steel that contains considerable undesired graphite as a result of the accidental addition of aluminum.

1-5.4 Grain Size

The prior-austenite grain size of high-carbon martensite steels, such as tool steels, can be assessed by comparing a fractured sample to a series of graded fractured specimens. The method is simple, accurate, and reproducible, and it is discussed in detail in Chap. 6.

1-5.5 Depth of Hardening

The depth of hardening in case-hardened steels, such as carbon tool steels, can be assessed through the use of fractured samples. The P-F (penetration-fracture) test developed by Shepherd is commonly used for evaluating carbon steel heats [31].

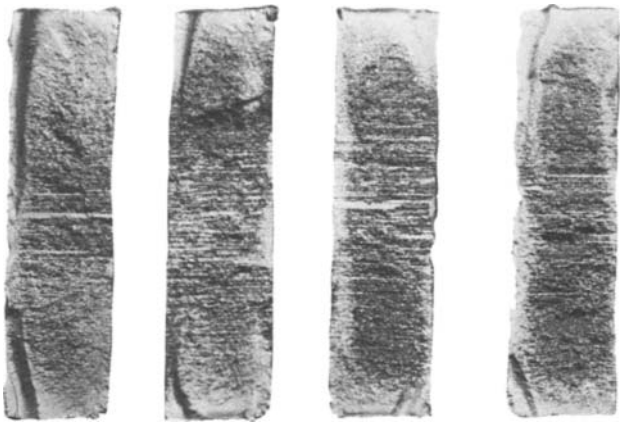

Figure 1-36 Fractograph of fractured hardened macroetched discs of AISI W1 (1.3% carbon) tool steel that were excessively graphitized as the result of a high, undesired aluminum content.

In this test, a ¾-in diameter, 4-in long sample is austenitized at the recommended temperature, quenched in brine, and fractured. The case depth is measured based on the change in fracture appearance. After fracturing, the surface is usually ground, etched, and its hardness tested to define the depth to a specific hardness.

1-5.6 Detection of Overheating

Fracture tests have also been used to detect overheating during soaking prior to hot working. In this test, a rectangular section, roughly 1-in square by 3 to 4 in long, is cut from the suspect material. It is normalized, quenched and tempered to 321 to 341 HB (Brinell hardness number), and fractured at room temperature. The appearance of coarse-grained facets on the fracture indicates overheating [32].

1-5.7 Evaluation of Quality

Fractures of longitudinal or transverse sections cut from wrought products or castings have been used for many years to evaluate metal quality. The fracture can reveal texture, flaking, graphitization, slag, blowholes, pipe, inclusions, and segregation. The general fracture appearance can be classified as coarse or fine, woody, fibrous, ductile, or brittle. Fibrous fractures result from microstructural anisotropy produced by alloy segregation or inclusions. Longitudinal fractures in wrought iron exhibit a classic fibrous appearance. Woody fractures generally result from gross alloy or nonmetallic segregations.

Fractures that occur during service or processing sometimes reveal features that indicate quality problems. Figure 1-37 shows a fractured case-hardened carbon steel bar that broke during heat treatment. The fine outer rim of the fracture reveals the depth of hardening. The central coarse-grained area indicates an unsound condition. Hot-acid etching of a disc cut from behind the fracture reveals a loose center and a segregated condition.

The fracture appearance of tensile test specimens has long been regarded as an index of quality. If the tensile test fracture does not have gross defects, its appearance is classified as irregular, angular, flat, partially cupped, or full cup-and-cone fracture. A full cup-and-cone fracture is generally regarded as the optimum fracture in the tensile test. Johnson and Fisher have conducted an extensive study of the fracture appearance of tensile bars and the relationship of the fracture to the test results [33]. For a given type of steel, such as normalized carbon steels or quenched and tempered alloy steels, there is an approximately linear relationship between tensile strength and tensile ductility.

The fracture test has been widely applied in the production of copper castings [34, 35]. The fracture test is often coupled with the removal of the gating or feeding portions of the casting. In copper-based castings, the color of the fracture provides considerable information [28]. The fracture color is influenced by alloy composition and the presence of various phases or constituents. A fracture of the alpha solid-solution phase of tin bronze appears red-brown, while a fracture of the tin-rich delta phase appears blue-white. Copper phosphide appears pale blue-gray, while lead appears dark blue-gray. Bronzes with low tin and phosphorus content are reddish brown. As the tin or phosphorus content is increased, the fracture appearance changes to gray-brown and then to gray. The addition of zinc in copper castings imparts a brassy yellow color to the fracture. Localized color variations in fractured copper-based castings indicate the presence of defects.

Figure 1-37 The fracture of this eutectoid carbon bar that broke during heat treatment reveals the depth of hardening and an unsound center condition. Hot-acid etching of a disc from behind the fracture reveals the unsound center and extensive segregation.

The texture of bronze fractures varies with compositions and grain size [28]. Increases in tin or phosphorus usually produce finer, silkier fractures, while lead additions produce a granular appearance. Bronzes with low tin contents often have a fibrous texture. Coarse-grained castings often exhibit coarse intergranular facets on the fracture, while chill-cast specimens usually exhibit fine fractures.

Considerable effort has been devoted to the study of fractures of red brass (ASTM B208). This work [34, 35] has shown that high-quality melts exhibit chill block fractures with at least 2 in of fine blue-gray structure and a columnar structure up to ¾ in from the chill face. Fractures of melts of intermediate quality have a coarser lighter blue-gray structure and less columnar depth and appear reddish rather than deep-blue. Fractures of low-quality melts have little clear blue-gray and columnar structure. These fractures may appear mottled because of a high gas content.

1-6 SPECIAL PRINT METHODS

A wide variety of special print methods have been developed to record deep-etched macrostructures, the distribution of oxide or sulfide inclusions, or the distribution of phosphorus or lead. Chemical spot tests have also been developed to identify the presence and location of a variety of chemical elements. Of these methods, only the sulfur print is used widely today.

1-6.1 Contact Printing

In a monumental work on the microscopic structure of iron and steel, Sorby described his method of "nature-printing" of deep-etched samples [1]. Sorby prepared blocks of metal which were "sufficiently well'bitten' with moderately strong acid to enable me to print with ink as from a wood block."

A contact print is made by rolling india ink on the surface of a deeply etched sample and pressing a piece of paper on this surface, being careful not to move the paper. Pressure is applied by a printing press or with a roller, and the paper is then peeled off. The method has been employed chiefly when photographic equipment is unavailable.

1-6.2 Sulfur Printing

The sulfur print technique is an exceptionally useful procedure for studying the heterogeneity of steels. During solidification, most of the impurities, such as sulfur and phosphorus, are rejected into the interdendritic liquid. Thus, the last areas to solidify become highly enriched in impurities. This phenomenon is used to advantage in macroetching, where the corrosion rate difference between the dendritic and interdendritic regions, segregate and matrix, and so forth allow the macrostructure to be observed.

Because the solubility of solid sulfur in iron is very low, nearly all the sulfur is precipitated as sulfide inclusions. Sulfide distribution is influenced by the steelmaking process, with the degree of deoxidation being a primary factor. In steels with a very high oxygen content (low carbon content, no strong deoxidizers), most of the sulfides are found in the central portion of the ingot. In steels with low oxygen contents (medium or high carbon content, additions of silicon, aluminum, etc.), the sulfides are more uniformly distributed.

The early history of the sulfur print method has been reviewed by Berglund [2]. The method used today was developed by Baumann in 1906, but a similar technique was developed by Heyn earlier in 1906. In Heyn's method, a piece of silk is placed on the ground steel surface and is moistened with a solution containing 10 g mercuric chloride, 20 mL hydrochloric acid, and 100 mL water. The solution attacks the sulfide inclusions, producing hydrogen sulfide gas, which reacts with the mercuric chloride, precipitating black mercuric sulfide on the silk. This results in a mirror image of the sulfide distribution on the face of the ground sample. It is claimed that the method also shows the distribution of phosphorus, but this claim has never been proven conclusively.

Baumann's method, which is being used today in preference to Heyn's method, employs ordinary photographic paper soaked in dilute sulfuric acid. The photographic paper should be thin so that good contact is achieved with the surface. While glossy papers produce sharper prints, they are slippery, and it is difficult to prevent blurring of the image. Consequently, matte finishes are preferred. Bromide-type papers are preferred to chloride-type papers.

To obtain good prints, a ground surface is required. Polished surfaces can be used but do not produce improved results. Indeed, paper slippage resulting in blurred images is more common with polished surfaces. The surface to be printed must be carefully cleaned; otherwise, dark spots will result. Many solvents commonly employed in the metallography laboratory are suitable for cleaning. It is not uncommon to read recommendations in the literature suggesting cleaning with gasoline, petroleum ether, or carbon tetrachloride. However, in the interest of safety in the laboratory, use of solutions of this type should be avoided. Instead cleaning with acetone, alcohol, or 1,1,1-trichloroethane is recommended.

Preetching the surface of steel samples with 10% nitric acid in water often helps to obtain quality sulfur prints. The preetch improves the image intensity and promotes contact adhesion. Steels with less than 0.010% sulfur give faint prints, and preetching produces a more distinct print. Preetched surfaces can be printed several times, whereas only one print can be obtained from ground surfaces of steels with normal sulfur levels. However, with resulfurized steels, the first print is usually so dark that all details are obscured, and a second print from the ground surface (no preetch) produces a better rendition of the sulfur distribution.

The photographic paper is soaked in a solution containing 1 to 5% sulfuric acid in water; a 2% solution is used most often. A more dilute solution can be used for resulfurized steels or for printing very large surfaces where some time is required to cover the sample with the paper.

In general, the paper is soaked for 1 to 5 min in the solution of dilute acid; a 3-

min soak is widely employed. Longer soaking times can cause swelling of the gelatin surface of the film, which produces poor results. After the soaking period, the excess solution is allowed to drip off the paper. Some metallographers lay the photographic paper on blotter paper to remove the excess solution. The surface of the photographic paper should be relatively dry before laying it on the steel surface in order to prevent image blurring.

The emulsion side of the paper is placed on the surface of the steel sample and left in contact for 2 to 10 min, depending on the sulfur content of the steel. The sulfuric acid reacts with the sulfide inclusions, producing hydrogen sulfide. Any bubbles under the paper from entrapped air or from hydrogen sulfide must be carefully moved off the edge of the sample using a roller, squeegee, or sponge. Care must be exercised so that the paper does not slide.

Several procedures have been used in placing the paper on the sample. Most commonly, the sample is placed on the workbench or in a vise, if the sample is small, with the ground surface upward. This technique has the advantage that air bubbles can be observed and removed. If air bubbles are not removed, white spots will be present on the print. Some prefer to lay the photographic paper with the emulsion side up on a glass plate and then press the ground surface onto the paper. Others prefer to use blotter paper rather than glass. With either of these procedures, the air bubbles cannot be observed and removed.

In general, the same contact time should be used for the majority of steel samples so that print intensities can be compared; 5 min is usually preferred. With resulfurized steels, a 2-min contact time is often preferred; for very low sulfur steels, a 10-min contact time is often used along with preetching. The entire process can be conducted under room illumination without damage to the paper. Strong sunlight, however, should be avoided.

After the contact time has elapsed, the print is peeled off carefully and examined. It is best not to handle the prints excessively before washing, fixing, washing, and drying. Washing is conducted in clear running water for about 15 min. The print is next fixed permanently in the usual photographic fixing solution for 15 to 20 min. This is followed by a second water wash for about 30 min. Finally, the prints are dried.

Such a print will clearly show the distribution of sulfur by the presence of darkly colored areas of silver sulfide. The print, of course, is a mirror image of the sulfur distribution in the sample. The chemical reactions occurring during sulfur printing are probably the following [36]:

$$(Fe,Mn)S_{(inclusion)} + H_2SO_4 \rightleftharpoons H_2S \uparrow + FeSO_4 + MnSO_4 \qquad (1\text{-}1)$$

$$H_2S + 2AgBr_{(emulsion)} \rightleftharpoons Ag_2S \downarrow + 2HBr \qquad (1\text{-}2)$$

The liberated hydrogen sulfide gas can become entrapped in voids or holes on the steel surface. Thus, when the paper covers these open areas, trapped hydrogen sulfide gas will often leave a brown color on the paper, indicating the presence of a gross sulfide segregate. In interpreting the sulfur print, one must recognize these areas as cracks or holes rather than sulfur segregation.

Sulfur print methods for fractured surfaces were developed by Rogers in 1912 and by Portevin in 1919, but the complexity of these methods has in general inhibited their use. There is need for a modern, simplified method for use in failure analysis.

Several investigators have used transparent films for sulfur printing. If transparent film is used, the print can be used to reproduce a reverse image of the sulfur print, and thus it is not necessary to photograph the sulfur print to make duplicates. O'Neill used a photomicrometer to examine his transparent sulfur prints and obtained quantitative measurements of sulfur content as a function of print density [37].

Farmer has developed a sulfur print method applicable to resulfurized copper alloys [38]. The standard method does not produce an image on resulfurized copper, even if a 10% sulfuric acid solution is used. The technique developed for free machining copper is similar to the standard method but incorporates an applied potential. The copper sample is ground and cleaned. The usual photographic bromide paper is soaked for 3 to 4 min in 2% aqueous sulfuric acid, and the excess acid is drained off. The emulsion side of the paper is placed on the

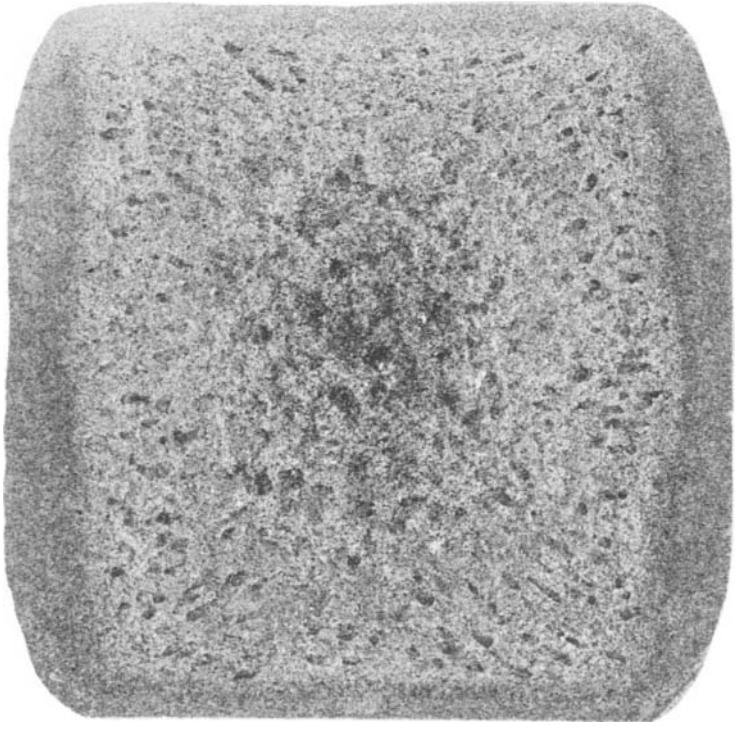

Figure 1-38 Mirror-image sulfur print of the macroetched disc shown in Fig. 1-6.

ground surface, and any air bubbles are removed. The specimen with the paper underneath is placed on an aluminum plate. The aluminum plate contacting the paper is connected to the positive terminal of a dc power supply, and the specimen is connected to the negative terminal. A potential of 3 V is applied for 10 s, producing an image of the sulfur distribution. The print is then removed and processed in the usual manner.

Figure 1-38 illustrates the use of sulfur prints in the study of macrostructures and shows a sulfur print of the macroetched disc presented in Fig. 1-6. Note that the sulfur print exhibits the same features as revealed by macroetching.

The intensity of sulfur prints can be influenced by chromium in the sulfides, a problem that was recognized in work with stainless steels. Monypenny, in his classic book on stainless steels, states that sulfur prints in stainless steels frequently do not show images [39]. In some of these stainless steel alloys that print poorly, the manganese content is about 0.20%, while chromium is 18% or greater. However if the manganese content in the stainless is 0.60% or greater, a print can be obtained. Garvin and Larrimore examined sulfur print response in AISI 430 stainless steel [40]. These authors made four ingots with 0.08, 0.42, 0.77, and 1.56% manganese. Low-manganese heats contained chromium sulfides and did not produce an image on the sulfur print. As the manganese content increased, print intensity increased. Figure 1-39 shows sulfur prints of discs cut from steels with two slightly different compositions but with the same sulfur content. On the right is a print of normal intensity in which little chromium is present in the sulfides, while on the left is a sulfur print which is considerably lighter because considerable chromium is present in the sulfides.

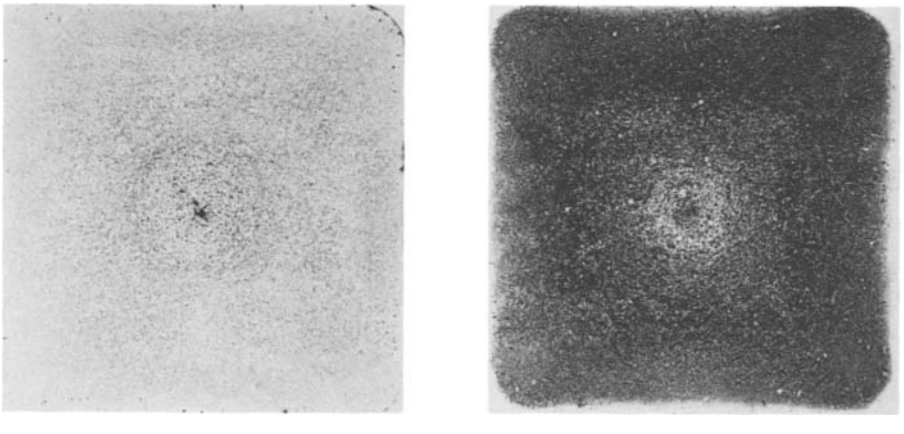

Figure 1-39 Sulfur print intensity is influenced by the composition of the sulfide inclusions. Both of the sulfur-printed discs shown contain 0.06% sulfur, but the print on the left is very light because most of the sulfides contain considerable chromium and are low in manganese content. The sulfides in the disc at the right contain very little chromium.

1-6.3 Oxide Printing

A technique for showing the distribution of oxide inclusions containing iron was developed by Niessner [41]. In this report it is claimed that a certain minimum amount of iron must be present in the oxides to obtain results, but the amount required was not determined. The original method is as follows: Gelatin paper is moistened in an aqueous solution containing 5% hydrochloric acid for about 5 min. The gelatinized side of the paper is blotted dry and pressed onto the polished surface of the steel sample for about 5 s. The paper is then removed and placed in an aqueous solution containing potassium ferrocyanide (20 g $K_4Fe(CN)_6$ to 1000 mL water). This solution develops the image. Potassium ferricyanide may also be used but at a lower concentration. The print exhibits a light-blue color over the contact area. Dark-blue spots are present at places where iron-containing inclusions were present.

Dienbauer modified the method by adding 15 g of sodium chloride to the dilute hydrochloric acid solution and by using photographic paper in place of gelatin paper [42]. These changes generally produced sharper images. It is claimed that both the sulfides and the iron-containing oxides are revealed on the same print with this procedure.

Grubitsch modified the oxide print method of Niessner by using cellophane film in place of gelatin paper [43]. This reportedly eliminated the air bubble problem, improved image sharpness, and permitted detection of small inclusions. Cellophane 0.025 mm thick is soaked for a few minutes in water. After the cellophane dries, a few drops of a 20% aqueous solution of quinoline-Etl are distributed over the surface of the film. After about a minute, the solution is wiped off. The film is placed on a polished sample, and an etching solution consisting of equal parts of a 1.2% ferrocyanide solution and a 0.25% hydrochloric acid solution is applied. After 2 to 2½ min, the etching solution is washed off and the film is removed and developed in a 2.5% solution of potassium ferrocyanide in water and then rinsed. The film image is next oxidized in a solution of 1 mL of 3% H_2O_2 in 100 mL water.

1-6.4 Phosphorus Printing

In addition to the chemical etchants that are claimed to reveal phosphorus segregation, a number of phosphorus printing methods have been developed. Canfield developed the first method for printing phosphorus segregation [44]. A sample with a ground surface is immersed in a solution consisting of 5 g $Ni(NO_3)_2$ plus 1.5 g $CuCl_2$ dissolved in 12 mL hot H_2O, 6 g $FeCl_3$, and 150 mL methanol (a few milliliters of HNO_3 may also be added). After 1½ to 3 min, a colored surface layer begins to form. This layer can exhibit a wide range of colors from pale brown to purplish red. Segregation shows up as white streaks or spots. This pattern can reportedly be transferred to photographic paper. A sheet of photographic paper is soaked for several minutes in a 5% solution of potassium ferricyanide in water. The paper is placed face up on blotting paper, and the coated steel surface is placed against the paper for about a minute. The paper is rinsed and fixed. The

segregated areas should show up as a blue color. Canfield states that the segregation is probably phosphorus, although this was not proved.

Another phosphorus print method was developed by Niessner [45] and is described by Feigl [46], Enos [47], and Kehl [48]. Two solutions, a soaking and a developing solution, are used. Niessner and Feigl state that filter paper is soaked in an ammonium molybdate–nitric acid solution (concentration not given). Enos, referencing the work of Niessner and Feigl, states that this solution should contain 5 g ammonium molybdate dissolved in 100 mL cold water, which is then added to 35 mL nitric acid. The excess solution is drained off, and the paper is placed on the surface of the sample. Niessner states that polished samples were used in his study. After a contact time of 3 to 5 min, depending on the phosphorus level, the paper is removed and placed in a developing solution. According to Niessner and Feigl, this solution consists of 50 mL $SnCl_2$, 50 mL HCl, and 100 mL H_2O. Since $SnCl_2$ is a powder rather than a liquid, we might assume that this is 50 mL of water saturated with $SnCl_2$. Enos and Kehl state that the developing solution is made by adding 5 mL of a saturated $SnCl_2$ solution to a mixture of 50 mL HCl and 100 mL H_2O. The paper is immersed in this solution for 3 to 4 min, and any iron salts and lower oxides of molybdenum that were absorbed by the paper dissolve. Initially, the print should appear yellow, but after about 45 s, a blue color is observed wherever phosphorus was present. Because the filter paper is attacked by the solution of $SnCl_2$ and HCl, a pinch of alum is added to the developer to harden the paper. After development, excess acid is washed off in flowing water and the paper is dried.

This author has tried this procedure using all possible mixtures but has been unable to obtain a useful print. With the procedure described by Enos and Kehl, a yellow color was obtained but not blue. Increasing the $SnCl_2$ content gave a strong blue color, but the resultant print was blotchy and devoid of any useful information. Canfield's method has also been tried, again, without useful results.

Phosphorus printing is rarely, if ever, performed today. Indeed, there is some question as to whether phosphorus distribution can be revealed by print methods. Since in general sulfur and phosphorus segregate in the same manner, segregation can be clearly revealed by the simple, proven sulfur print method. In steels with a very low sulfur content, a phosphorus print would be useful.

1-6.5 Lead Printing and Exudation Test

Lead, which is added to steels to improve machinability, requires special attention by the steelmaker in order to obtain a uniform distribution of the lead. Because of the potential variability in the distribution of lead, macroscopic testing is a key tool in quality control. Three techniques are available for revealing the lead distribution—macroetching, lead printing, and lead exudation. The latter technique, frequently referred to as the lead "sweat" test, is the most frequently used because of its simplicity.

Bardgett and Lismer developed an electrolytic etching technique that reveals lead segregation [49]. The disc is cleaned and electrolytically etched in a solution

of ammonium acetate, which can be prepared using either of the following procedures:

Method A: 50 g ammonium acetate
1000 mL water

Method B: 75 mL glacial acetic acid
900 mL water
Addition of ammonium hydroxide until the solution is just alkaline

The solution is placed in a stainless steel container which is attached to the positive terminal of a 6-V battery. The billet disc is placed on the bottom of the vessel, surface upward. A platinum wire loop extending across the surface is attached to the negative terminal of the battery and is suspended about ¼ in above the sample surface in the solution. The loop is moved around above the surface for 30 to 60 s. The location of lead segregates are shown by the formation of a sharp brown stain.

Lead print methods can also be used to reveal the lead distribution. Volk used gelatin paper soaked in concentrated acetic acid [50]. The paper is placed on the surface of the disc for about 1 min. It is then removed and placed in water saturated with hydrogen sulfide for about 2 to 3 min. The location of the lead is indicated by brown spots of lead sulfide on the gelatin paper.

Northcott and McLean used a lead print method developed by Ledloy, Ltd. [51]. Three solutions are required:

Solution	Components
Printing solution	25 g tartaric acid 100 g ammonium acetate 250 mL water
	Saturation of resulting solution with H_2S
Developing solution	Water saturated with H_2S
Clearing solution	10% aqueous ammonium persulfate or tartaric acid solution saturated with H_2S.

The ground billet disc is first etched with an aqueous solution of 50% HNO_3, washed, and dried. Gelatin paper is soaked in the printing solution and then placed on the surface of the disc. The back of the paper is kept moist with the printing solution. After 2 to 3 min, the paper is removed and placed in the developing solution. Intense black staining due to dissolved iron is observed. Some of this black stain is removed in the developing solution and the balance in the clearing solution. After clearing, the print is washed in clean developing solution to counter fading. The print is then washed in water, rinsed with alcohol, and dried.

Bardgett and Lismer developed an electrographic method of lead printing using caustic soda as the printing solution and sodium sulfide as the developing solution. However, they later found that a method suggested to them by Wragge, which uses gelatin paper soaked in an 10% ammonium acetate solution, was better [49]. The excess solution is drained off, and the paper is placed, gelatin side upward, on a double layer of blotter paper. The blotter paper has been previously soaked in the same solution and rests on a flat aluminum plate that is attached to the negative terminal of a battery or power supply. The surface of the sample is pressed into the gelatin surface. A smooth ground surface can be employed, but results are best using a polished specimen. A small brass plate, which is connected to the positive terminal of the power source, is placed on the back of the disc. A voltage of about 2 V/in^2 of surface is applied for about 2 min. The power is then turned off, and the gelatin paper is placed in an aqueous 5% ammonium acetate solution for 30 s. A small quantity of water saturated with tartaric acid should be added to the ammonium acetate solution. Next, the paper is washed and soaked in a weak aqueous hydrogen sulfide solution until the print details are revealed adequately. The hydrogen sulfide solution should not be near enough to the ammonium acetate solution for contamination to occur.

The iron-staining problem encountered with the use of ammonium acetate solutions can be eliminated by the use of dilute caustic acid solutions, as developed by Wragge [52]. In this method a desilvered matte-type printing paper, a toughened fine-grained filter paper, or a smooth-surfaced gelatinized white blotter paper can be used. Both ferrous and nonferrous leaded metals can be printed using Wragge's procedure. For either metal, the surface should be ground and macroetched. The printing paper is immersed in a 5% aqueous NaOH solution for about 2 min, lightly dried between blotter papers, and placed on the metal surface. Air bubbles should be removed. A contact time of 2 min is adequate for both steel and brass specimens. The paper is removed and developed for a few seconds in a freshly prepared 5% aqueous sodium sulfide solution. Prints made on steel specimens should be washed for 10 to 15 min before drying. For copper alloys, a slight brown stain on the print can be removed after development by soaking the print about 15 s in an aqueous 10% potassium cyanide solution. The print can then be washed and dried. Figure 1-40 shows an example of lead distribution in a leaded free-machining steel, revealed using either Wragge's printing method or the sweat test.

The lead exudation test is the most commonly employed technique for detecting lead segregation [49]. The billet disc is coated with a thin layer of light oil and heated in a small furnace to 1290°F (699°C). The disc is held at temperature for 10 min for each inch of thickness. A minimum thickness of 2 in is usually recommended. Globules or beads of lead will exude from the steel wherever lead is segregated.

To evaluate the degree of lead segregation, the disc is compared to a set of standards, such as shown in ASTM Specification A582. The applicable ASTM standard or a customer-manufacturer agreed-on limit is used as the acceptance or rejection criterion. If the billet disc exhibits a rejectable condition, a portion

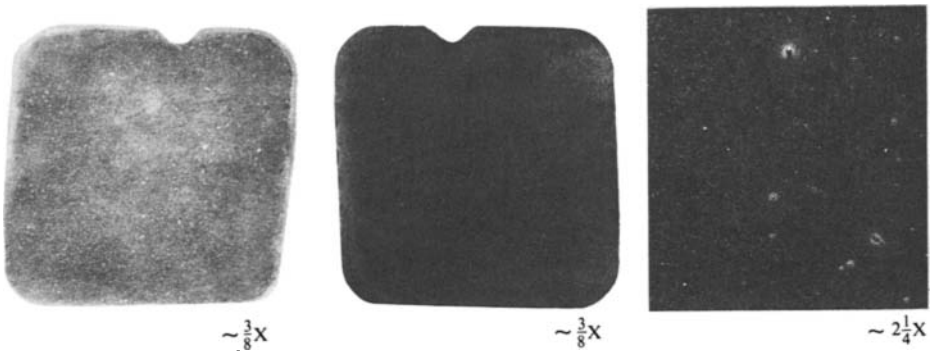

Figure 1-40 Wragge's lead print method (left) and the lead sweat test (center) were used to reveal the lead distribution in this free-machining steel billet disc. A few small spots of lead segregation were detected (right), otherwise the lead distribution was quite uniform.

adjacent to the disc is scrapped and another disc is tested. This process is repeated, as required, until the segregation is removed. Lead segregation is most commonly encountered at the bottom end of the ingot.

Bardgett and Lismer studied lead exudation using hot-stage microscopy [49]. A sample from a region containing lead segregation was photographed with a cine camera during heating and the resulting photographs reveal that a small amount of lead exudation occurred at temperatures as low as 86°F (30°C). When the samples reached 455 to 464°F (235 to 240°C), lead beads suddenly spurted out onto the sample surface. At 662 to 752°F (350 to 400°C) the beads spread out over the surface and coalesced. Chemical analysis of the beads showed that they were 98 to 99% lead (Pb). Heating above 464°F (240°C) caused the bright metallic beads to oxidize, with the color changing from bright red to yellow and finally to gray. These results showed that exudation occurs at temperatures well below the melting point of lead, which is about 621°F (327°C).

The exudation test has also been used to evaluate steels treated with bismuth, another low-melting-point metallic additive used to improve machinability. Bismuth melts at about 520°F (271°C), which is about 100°F lower than the melting point of lead. Exudation tests on bismuth-treated steels are performed at about 1200°F (649°C).

1-6.6 Miscellaneous Print Methods

Singleton has described a simple test for evaluation of mill scale removal after shot blasting [53]. The test is performed immediately after shot blasting, and the surface should be free of loose rust, dust, oil, grease, etc. A solution of copper sulfate is applied to the surface, causing copper to deposit on areas free of mill scale. Any remaining patches of mill scale appear as dark areas against the copper background. These areas are compared to a standard set of illustrations to assess the amount of mill scale remaining on the surface. The test solution consists of a mixture of aqueous 4% anhydrous copper sulfate in 1% sulfuric acid. A small

addition of a wetting agent, such as Teepol, is recommended. Since the solution is poisonous and contains a strong corrosive acid, it should be handled carefully.

Picard and Greene have described printing methods to detect contamination of metallic surfaces by foreign metals that results from machining, brushing, and/or accidental contact [54]. Using this method, these authors have detected iron contamination on the surfaces of nickel, titanium, and zirconium and copper contamination on stainless steel. For printing, they use either desilvered unexposed or exposed single-weight Polycontrast photographic paper. The choice of exposed or unexposed paper depends on the color of the precipitate formed. If a light precipitate is formed, black exposed paper provides the best contrast. Exposed paper was used to reveal porosity in a number of metallic coatings. The test is performed as follows: The paper is saturated in the appropriate electrolyte solution and placed on the test surface. After an appropriate time, it is placed in a developing solution, rinsed in distilled water, and dried. For steels, including stainless steel, they employed a 5 wt % Na_2SO_4 solution as the electrolyte, and for copper-clad aluminum, they used a 3 wt % NaCl solution as the electrolyte.

Hunter et al. have described electrographic print tests that employ procedures used in colorimetric spot testing for the detection of a variety of metals [55]. In this method, gelatinized paper (e.g. desilvered photographic paper) is soaked in an appropriate electrolyte and placed on an aluminum block. The specimen is placed on the paper, and pressure is applied. Current from a 6-V battery is applied, with the aluminum block as the cathode and the sample as the anode. An ammeter is used to measure the current flow to ensure rapid dissolution. The current required depends on the size of the sample, the element to be detected, and the electrolyte chosen. In general, application of the current for 30 s was adequate. These authors have used this procedure for detecting a wide variety of inclusion types in many different metals, for alloy identification, and for detecting porosity in metallic coatings.

1-7 SUMMARY

This chapter has presented information pertaining to the visualization and interpretation of the macrostructure of metals. These techniques permit examination of a large number of materials using either nondestructive or destructive methods. When areas of questionable quality are detected, microscopic analysis may be desired to more clearly identify the nature of the problem. Thus, macrostructural examination is often the prelude to microscopic examination. Macroscopic examination is clearly a fundamental step in both quality control and failure analysis.

REFERENCES

1. Sorby, H. C.: "On the Microscopical Structure of Iron and Steel," *J. Iron Steel Inst.*, pt. 1: 1887, pp. 255–288.
2. Berglund, T.: *Metallographers' Handbook of Etching,* Sir Isaac Pitman & Sons, Ltd., London, 1931.

3. Gill, J. P., and H. G. Johnstin: "Deep Acid Etch Test. An Interpretation for Tool Steels," *Met. Prog.*, vol. 22, September 1932, pp. 37–42.
4. Yatsevitch, M. G.: "Essential Factors in Conducting the Macroetching Test under Usual Practical Conditions of Production Work," *Trans. Am. Soc. Steel Treat.*, vol. 21, 1933, pp. 310–342.
5. Magnusson, E.: "Primary Etching of Welds," *Jernkontorets Ann.*, vol. 131, no. 6, 1947, pp. 212–224.
6. Pokorny, A.: "The Influence of the State of the Surface on the Etching Effect," *Prakt. Metallogr.*, vol. 17, 1980, pp. 23–28.
7. Buhr, R. K., and F. Weinberg: "Etching Steel to Determine Phosphorus Segregation," *J. Iron Steel Inst.*, vol. 205, 1967, pp. 1161–1164.
8. Karl, A.: "Investigations into the Suitability of the Oberhoffer Etch for Identifying Surface Defects," *Prakt. Metallogr.* vol. 15, 1978, pp. 469–485.
9. Koster, W.: "Effects of Nitrogen in Technical Iron," *Arch. Eisenhuettenwes,* vol. 3, 1930, pp. 637–658.
10. MacGregor, C. W., and F. R. Hensel: "The Influence of Nitrogen in Mild Steel on the Ability of Developing Flow Layers," *J. Rheology,* vol. 3, 1932, pp. 37–52 (see abstract in *Metals and Alloys,* vol. 3, May 1932, pp. 127–128).
11. Bish, R. L.: "A Method of Revealing Deformation in Mild Steel," *Metallography,* vol. 11, 1978, pp. 215–218.
12. Bish, R. L.: "The Action of Fry's Reagent on Steel," *Metallography,* vol. 12, 1979, pp. 147–151.
13. Giedenbacher, G., and F. Sturm: "Deformation Zones in Notched Flat Tensile Specimens," *Prakt. Metallogr.*, vol. 15, 1978, pp. 3–10.
14. Weinberg, F., and R. K. Buhr: "Solidification Studies of Steel Castings," *Iron Steel Inst., London, Spec. Rep. 110,* 1968, pp. 295–304.
15. Alexander, B. H., and F. N. Rhines: "Dendritic Crystallization of Alloys," *Trans. Am. Inst. Min. Metall. Eng.*, vol. 188, 1950, pp. 1267–1273.
16. Dawson, J. V., and W. Oldfield: "Euctectic Cell Count - An Index of Metal Quality," *BCIRA J.*, vol. 8, no. 2, 1960, pp. 221–231.
17. Adams, R. R.: "Cast Iron Strength vs. Structure," *Trans. Am. Foundrymen's Soc.*, vol. 50, 1942, pp. 1063–1103.
18. Merchant, H.D.: "Metallography of Eutectic Cells in Cast Iron," *Foundry,* vol. 91, 163, pp. 59–65.
19. Boyles, A.: *The Structure of Cast Iron,* American Society for Metals, Cleveland, 1947.
20. Merchant, H. D.: "Eutectic Cells in Cast Iron. Structure and Delineation," *Trans. Am. Foundrymen's Soc.*, vol. 70, 1962, pp. 973–992.
21. Beck, P. A., et al.: "Grain Growth in High-Purity Aluminum and in an Aluminum-Magnesium Alloy," *Trans. Am. Inst. Min. Metall. Eng.*, vol. 175, 1948, pp. 372–400.
22. Beck, P. A., M. L. Holzworth, and P. R. Sperry: "Effect of a Dispersed Phase on Grain Growth in Al-Mn Alloys," *Trans. Am. Inst. Min. Metall. Eng.*, vol. 180, 1949, pp. 163–192.
23. Ryvola, M: "Rapid Way to Determine Aluminum Grain Size," *Met. Prog.*, vol. 105, June 1974, pp. 80–81.
24. Benson, D. K.: "Residual Stress Measurement in Steels Using a Chemical Etchant," *Metall. Trans.*, vol. 3, 1972, pp. 2547–2550.
25. Vander Voort, G. F.: "Macroscopic Examination Procedures for Failure Analysis," *Metallography and Failure Analysis,* Plenum Press, New York, 1978, pp. 33–63.
26. Ljunggren, B. O. W. L.: "Method of Sclero-Grating Employed for the Study of Grain Boundaries and of Nitrided Cases; Grain Structures Revealed by Cutting," *J. Iron Steel Inst.*, vol. 141, 1940, pp. 341p–404p.
27. Clarebrough, L. M., and G. J. Ogilvie: "Development of the Macrostructure of Metals by Machining," *Machining-Theory and Practice,* American Society for Metals, Cleveland, 1950, pp. 110–122.
28. Hanson, D., and W. T. Pell-Walpole: "Methods of Assessing the Quality of Cast Bronzes," *Chill-Cast Tin Bronzes,* Edward Arnold, London, 1957, pp. 22–55.

29. Enos, G. M.: "Fractures," *Visual Examination of Steel*, American Society for Metals, Cleveland, 1940, pp. 37–54.
30. Ostrofsky, B.: "Materials Identification in the Field," *Mater. Eval.*, vol. 36, August 1978, pp. 33–39, 45.
31. Shepherd, B. F.: "The P-F Characteristic of Steel," *Trans. Am. Soc. Met.*, vol. 22, 1934, p. 979–1016.
32. Strohm, J. R., and W. E. Jominy: "High Forging Temperatures Revealed by Facets in Fracture Tests," *Trans. Am. Soc. Met.*, vol. 36, 1946, pp. 543–571.
33. Johnson, H. H., and G. A. Fisher: "Steel Quality as Related to Test Bar Fractures," *Trans. Am. Foundymen's Soc.*, vol. 58, 1950, pp. 537–549.
34. Baker, F. M., C. Upthegrove, and F. B. Rote: "Melt Quality and Fracture Characteristics of 85-5-5-5 Red Brass," *Trans. Am. Foundrymen's Soc.*, vol. 58, 1950, pp. 122–132.
35. French, A. R.: "Melt-Quality Test for Copper-Base Alloys," *Foundry Trade J.*, vol. 98, 1955, pp. 253–257, 281–293.
36. Poole, S. W., and J. A. Rosa: "Segregation in a Large Alloy-Steel Ingot," *Trans. Am. Inst. Min. Metall. Eng.*, vol. 162, 1945, pp. 459–473.
37. O'Neill, H.: "Quantitative Printing Methods for the Study of Segregation in Steel," *Metallurgia*, vol. 45, 1952, pp. 215–216.
38. Farmer, J. S.: "Sulphur Printing of High-Sulphur Copper," *Met. Mater.*, June 1979, p. 35.
39. Monypenny, J. H. G.: *Stainless Iron and Steel*, vol. 2, 3d ed., revised, Chapman and Hall, Ltd., London, 1954, p. 96.
40. Garvin, H. W., and R. M. Larrimore: "Metallurgical Factors Affecting the Machining of a Free Machining Stainless Steel," *Mech. Working of Steel*, 11, Met. Soc. Conf., vol. 26, American Institute of Mining, Metallurgical and Petroleum Engineers, 1965, pp. 133–150.
41. Mitsche, R.: "The Detection of Oxide Inclusions in Steels by Imprints," *Berg Huettenmaenn Jahr.*, vol. 83, 1935, pp. 127–133.
42. Dienbauer, H., and R. Mitsche: "Metallographic Printing Methods," *Berg Huettenmaenn Jahr.*, vol. 86, 1938, pp. 33–35.
43. Grubitsch, H.: "The Use of Cellophane in the Oxide Print Method of Niessner," *Arch. Eisenhuttenwesen*, vol. 16, August 1942, pp. 79–80.
44. Canfield, R. H.: "Phosphor Prints. A New Method of Detecting Phosphorus Segregations in Steel," *Chem. Metall. Eng.*, vol. 30, no. 12, 1924, p. 470.
45. Niessner, M.: "New Methods for Chemical Identification of Alloying Additions and Nonhomogenieties in Metallic Materials," *Mikrochemie*, vol. 12, 1932, pp. 1–24.
46. Feigl, F.: *Spot Tests*, vol. 1, 4th ed., Elsevier Publishing Company, New York, 1954, pp. 426–427.
47. Enos, G. M.: *Visual Examination of Steel*, American Society for Metals, Cleveland, 1940.
48. Kehl, G. L.: *The Principles of Metallographic Laboratory Practice*, 3d ed., McGraw-Hill Book Company, New York, 1949.
49. Bardgett, W. E., and R. E. Lismer: "Mode of Occurrence of Lead in Lead-Bearing Steels and the Mechanism of the Exudation Test," *J. Iron Steel Inst.*, vol. 151, pt. 1, 1945, pp. 281p–301p.
50. Volk, K. E.: "The Metallographic Proof of Pb in Steel," *Arch. Eisenhuettenwesen*, vol. 16, 1942, pp. 81–84.
51. Northcott, L., and D. McLean: "The Structure and Segregation of Two Ingots of Ingot Iron, One Containing Lead," *J. Iron Steel Inst.*, vol. 148, 1943, pp. 429p–439p.
52. Wragge, W. B.: "'Lead Printing' Ferrous and Non-Ferrous Metals," *Metallurgia*, vol. 32, May 1945, pp. 3–6.
53. Singleton, D. W.: "A Simple Test for the Detection of Residual Millscale on Shotblasted Steel Surfaces," *Iron Steel*, vol. 41, January 1968, pp. 17–19.
54. Picard, R. J., and N. D. Greene: "Detection of Surface Contamination by Corrosion Printing," *Corrosion*, vol. 29, 1973, pp. 282–284.
55. Hunter, M. S., J. R. Churchill, and R. B. Mears: "Electrographic Methods of Surface Analysis," *Met. Prog.*, vol. 42, 1942, pp. 1070–1076.